Applied Thermal Engineering 290 (2026) 130132

Contents lists available at ScienceDirect

Applied Thermal Engineering

journal homepage: www.elsevier.com/locate/apthermeng

Research Paper

Utilizing aqua-ammonia as a clean and scalable fuel in steam power plants

Ramin Mehdipour [a], Zahra Baniamerian [a,*], Hassan Ali Ozgoli [b], Seamus Garvey [a], Alasdair Cairns [a], Agustin Valera-Medina [c], Sivachidambaram Sadasivam [c], Bruno Cardenas [a]

[a] University of Nottingham, Nottingham, UK
[b] Macquarie University, Sydney, NSW, Australia
[c] Cardiff University, Cardiff, UK

ARTICLE INFO

Keywords:
Aqua-ammonia
Steam power plants
Clean fuel
Water-energy nexus
Thermodynamic modelling

ABSTRACT

Global electricity generation continues to rely heavily on fossil fuels, with coal as the largest single source and natural gas (NG) contributing a substantial, second-largest share. To decarbonize this sector, hydrogen and ammonia are being explored as alternatives to natural gas; however, both face significant challenges. Safe and cost-effective transportation of hydrogen remains unresolved, while ammonia is limited by issues of toxicity and corrosiveness. This study proposes and evaluates the use of aqua-ammonia (A-A)—a liquid mixture of ammonia and water—as a novel fuel for decarbonizing steam power plants. A-A offers key advantages over hydrogen and pure ammonia, including safer transport, reduced corrosiveness and toxicity, and compatibility with existing NG infrastructure. Despite these advantages, its potential as a large-scale fuel for power generation has not been explored in the open literature, and no prior work has assessed its integration across production, transmission, separation, and combustion stages. This work explicitly addresses this research gap by evaluating A-A as a fully integrated energy carrier for utility-scale steam power plants and by introducing the concept of simultaneous energy and water delivery through a single pipeline—an aspect absent from previous studies. Given that A-A is a clean fuel capable of transporting both energy and water simultaneously through a single pipeline, this research demonstrates that A-A can offer solutions to two critical challenges: (1) providing a clean, safe, and practical alternative fuel to fossil fuels, and (2) supplying the required water for power plants operation — which is one of the most significant barriers to the development of steam power plants and a pressing issue in regions suffering from water scarcity. The study provides the first thermodynamic assessment of a full-scale Rankine cycle operating on ammonia extracted from A-A, modelling of a 200 MW Rankine cycle plant, powered by ammonia extracted from A-A, using Engineering Equation Solver (EES). The base case achieved a gross thermal efficiency of 41.26% and net efficiency of 35.07%, surpassing comparable NG-fired plants. The model evaluates multiple operational parameters—boiler pressure, condenser pressure, extraction pressures, and off-design operation—to identify optimal conditions. A 15% ammonia concentration in A-A is found to triple the volumetric energy delivery compared to NG at typical pipeline pressures, while simultaneously supplying sufficient water to meet plant cooling and process demands. Separation of ammonia from water is examined via three methods: Full evaporation, ammonia boiling-based, and membrane, with the latter demonstrating the best integration with condenser heat recovery and minimal efficiency penalty (~1.2%). Lifecycle analysis indicates potential for near-zero CO_2 emissions using green ammonia, with total annual fuel demand estimated at 773,000 t. Overall, this study establishes—for the first time—the technical feasibility, infrastructural compatibility, and environmental viability of A-A as a next-generation energy carrier for low-carbon power generation.

1. Introduction

Rising global temperatures, recurrent droughts, and widespread pollution from fossil fuel consumption have intensified the need for a global energy transition. Decarbonization of the power sector, which remains heavily dependent on natural gas (NG), coal, and petroleum, is considered essential for achieving climate targets by 2050.

Recent efforts to decarbonize the power sector have leveraged advances in materials science, multiphase heat transfer approaches and nanotechnology to improve thermal management, heat transfer, and

* Corresponding author.
E-mail address: zahra.baniamerian@nottingham.ac.uk (Z. Baniamerian).

https://doi.org/10.1016/j.applthermaleng.2026.130132
Received 6 October 2025; Received in revised form 24 December 2025; Accepted 3 February 2026
Available online 5 February 2026

renewable energy system performance. For example, graphene-based polymer composites have been developed to enhance thermal conductivity and heat dissipation in demanding thermal applications [1]. Similarly, nanofluids—fluids containing dispersed nanoscale particles—have demonstrated significantly improved heat transfer and storage characteristics, showing promise for energy systems aiming to enhance thermal efficiency and sustainability [2–6]. Boiling-mode heat transfer has also contributed significantly to enhancing thermal efficiencies [7–10]. These advances underscore a broader shift toward integrating advanced materials and fluid technologies in clean energy applications [11,12].

Furthermore, researchers and policymakers have also increasingly focused on alternative fuels that can reduce or eliminate carbon emissions from thermal power generation.

Hydrogen has been widely proposed as a clean energy carrier, particularly in the heating and power generation sectors. However, despite its promise, hydrogen adoption faces substantial barriers. These include challenges in storage [13,14], transportation infrastructure [15], and elevated NO_x emissions during combustion [16]. Partial substitution of NG with hydrogen blends has been explored [17,18], but the resulting reduction in carbon emissions is modest and insufficient for long-term decarbonization targets.

Ammonia offers several advantages over hydrogen, including superior energy density [19], lower costs of production and handling [20], and greater ease of liquefaction and transport. Furthermore, it can serve both as a fuel and as a hydrogen carrier [21,22]. Recent studies have demonstrated ammonia's potential in gas turbines and internal combustion engines [23,24], as well as in co-firing applications with NG. Research into ammonia combustion characteristics [25,26] and its role as a hydrogen carrier [20,21] further supports its viability in a low-carbon energy landscape.

However, ammonia's potential as an energy carrier is hindered by its inherent toxicity and corrosiveness, which pose serious operational and safety concerns [27]. These risks become particularly critical in pipeline systems, where a drop in pressure—especially below 12 bar—can lead to phase changes that cause ammonia to vaporize. This not only increases the risk of toxic exposure but also accelerates material degradation. As a result, the practical deployment of ammonia, especially in repurposed pipeline infrastructure, remains challenging. Recent studies have highlighted the need for corrosion-resistant materials and comprehensive safety measures to address the long-term impacts of ammonia transport [27–30].

An innovative solution to mitigate these limitations involves dissolving ammonia in water to form aqua-ammonia (A-A), a stable liquid under atmospheric conditions. Water acts as a natural absorbent for ammonia, significantly reducing its vapor pressure, toxicity, and corrosiveness. Water significantly reduces ammonia's volatility and corrosiveness, making A-A safer to handle and more compatible with conventional infrastructure. This solution not only offers improved handling safety but also enhances energy storage and transmission feasibility, as it behaves similarly to water in pipelines and can be transported at low pressures (1–4 bar). Importantly, A-A can be stored in atmospheric tanks and integrated into existing NG infrastructure, enabling scalable, cost-effective, and practical deployment in power plants—a gap not addressed in prior literature.

Water consumption in steam power plants is one of the major environmental and operational challenges in the power generation industry. These plants consume significant amounts of water primarily for cooling the exhaust steam from turbines, with much of this water lost through evaporation in cooling towers and thus unrecoverable. In regions facing water scarcity, securing the necessary water for continuous plant operation can create competition between the energy sector and other critical water consumers such as agriculture and domestic use. Although the water used within the boiler operates in a closed-loop cycle with minimal loss, cooling processes remain the dominant factor contributing to high water consumption in steam power plants. In many regions, this issue has become a bottleneck for the development, establishment, and even continued operation of such power plants, and there are documented cases of steam power plant shutdowns around the world due to water crises.

Ammonia–water mixtures are key working fluids in both Kalina and Goswami cycles due to their favorable thermophysical properties for low-grade heat recovery. Shahrokhi et al. [31] performed a comparative analysis of dual Kalina cycle configurations for recovering heat from the boiler stack in a steam power plant and found that the optimized configuration improved plant efficiency by up to 11.3% compared to conventional systems, while also lowering exergy destruction in the heat recovery process. In a separate study, Hosseinpour et al. [32] investigated the integration of Organic Rankine, Kalina, and Goswami cycles as bottoming options for a combined biomass gasifier–gas turbine cycle. Their results showed that the Kalina and Goswami cycles outperformed the ORC in terms of net power output and exergy efficiency, with the Goswami cycle offering the highest performance despite its operational complexity. Further, Hosseinpour et al. [33] evaluated the partial substitution of fossil fuels with biomass gasification in a conventional combined power plant integrated with a Kalina cycle and demonstrated that the proposed configuration could reduce fossil fuel consumption by up to 38% while maintaining competitive thermal performance, thereby supporting the transition toward cleaner power generation.

The use of A-A for heating and as a fuel was first introduced by Mehdipour et al. in reference [34], where a fuel transmission network similar to potable water distribution systems was proposed. This article investigates the feasibility of repurposing existing gas pipelines for the transportation of this fuel. Prior to this study, the repurposing of gas pipelines for water transport (noting that A-A has physical similarities to water) in ice-source heat pump systems was examined in references [35–38].

Although literature on A-A has primarily focused on thermodynamic properties as a refrigerant [39–41], organic Rankine cycles [42,43], or NO_x reduction, its potential as a primary fuel for large-scale power generation remains unexplored. This gap is significant: prior work has neither assessed A-A's viability as a standalone fuel nor analysed its integration within utility-scale steam power systems. The combined advantages of safer low-pressure transport, dual energy–water delivery, and compatibility with Rankine-cycle operation have not been assessed in any previous publication. However, despite substantial progress on ammonia- and hydrogen-fuelled power plants, the safe and economically viable transport of these fuels remains an unresolved challenge. Building on these gaps, the present work investigates the integration of A-A into a full-scale power generation system—from production and transport to ammonia–water separation and combustion—evaluating both infrastructure feasibility and thermodynamic performance.

This study addresses the identified research gap by evaluating the feasibility of A-A for full-scale power generation. Specifically, it investigates: (1) preparation and transport of A-A through existing pipelines, (2) separation of A-A to water and ammonia and combustion of ammonia for power generation, and (3) the dual utility of A-A in supplying both fuel and process water for steam power plants. By combining thermodynamic modelling, infrastructure assessment, safety analysis, and environmental impact evaluation, the study provides a comprehensive assessment of A-A's potential as a next-generation sustainable fuel.

The main significance of this work compared to existing literature is that it provides the first integrated evaluation of aqua-ammonia as a complete fuel system—from production and transport to separation and combustion—while simultaneously introducing the dual energy–water delivery concept. No prior study has assessed A-A's pipeline compatibility, thermodynamic performance in utility-scale steam cycles, or its capability to eliminate water scarcity barriers in thermal power plants. The study presents a thermodynamic model of a 200 MW Rankine cycle powered by ammonia extracted from A-A and evaluates technical, economic, and environmental aspects, providing a foundation for large-

scale implementation of this innovative fuel system for power generation.

2. A-A in context

2.1. Safety and corrosion considerations

A-A in practice is the diluted ammonia concentration that significantly reduces corrosiveness. Empirical studies have shown that low-concentration A-A does not corrode materials such as carbon steel and stainless steel under ambient conditions. Furthermore, its behaviour under low pressure closely resembles that of water, allowing it to be transported in standard water-grade pipes, including polyethylene (PE), polyvinyl chloride (PVC), and other non-metallic materials.

The suppression of ammonia's high vapor pressure through dilution prevents phase change under normal pipeline conditions, thus eliminating the need for complex pressurization or cryogenic containment systems. The presence of water also stabilizes thermal gradients and reduces the risk of localized material degradation, which is commonly observed in pure ammonia systems under fluctuating temperature conditions.

Additionally, A-A's relatively low flammability and low explosion risk make it more suitable for use in populated areas than NG or hydrogen. While there is an explosive limit of 5.3–15% by volume for NG and 15–28% by volume for ammonia, A-A is not at all explosive. Although, ammonia combustion requires precise air-fuel mixing and ignition control, A-A can be separated into ammonia and water just before combustion, thus confining the risks to a controlled environment.

2.2. Transport infrastructure compatibility

One of the most compelling features of A-A as a fuel is its compatibility with existing NG transmission networks. Unlike hydrogen, which requires substantial modification due to its low molecular weight, high diffusivity, and tendency to cause metal embrittlement, A-A behaves similarly to water. This allows the reuse of NG pipeline networks for its distribution with minimal modifications.

At operating pressures typical of city gas distribution systems (0.2–13 bar gauge), A-A maintains a stable liquid phase. This characteristic enables a volumetric energy transport capacity up to 2.8 times greater than NG at 15% ammonia concentration. In higher-pressure intercity pipelines (above 20 bar), A-A remains practical and significantly safer than pure ammonia, which may liquefy under these conditions but requires more stringent safety measures.

2.3. Energy capacity of repurposed pipelines for alternative fuels

One critical aspect of repurposing existing NG pipelines for alternative fuels is assessing the deliverable energy capacity for each alternative. A robust comparison requires evaluating the energy transfer capabilities of alternatives relative to NG. It evaluates the maximum energy capacity of the current infrastructure for each fluid. It is based on the maximum feasible velocity within the pipeline for each fuel. To quantify this, we define an Energy Ratio (ER), which compares the energy transfer capability of alternative fuels $\dot{E}_{\mathrm{alt}}$ to NG, $\dot{E}_{\mathrm{NG}}$. ER is calculated as:

$$\mathrm{ER} = \frac{\dot{E}_{\mathrm{alt}}}{\dot{E}_{\mathrm{NG}}} = \frac{\rho_{alt}\boldsymbol{v}_{\boldsymbol{max,alt}}A(HV)_{alt}}{\rho_{NG}\boldsymbol{v}_{\boldsymbol{max,NG}}A(HV)_{NG}} \tag{1}$$

where, ρ is density, $\boldsymbol{v}_{\boldsymbol{max}}$is the maximum allowable velocity [44], A is the pipeline cross-sectional area, and HV is the heating value.

Fig. 2 compares the ER of various concentration of A-A with hydrogen, pure ammonia and NG. The horizontal axis represents pressure levels corresponding to different parts of transportation pipelines. The black dashed line at ER = 1 serves as a benchmark, indicating parity with the energy delivery performance of NG in existing infrastructure.

As shown in the plots, an A-A concentration of just 6% can deliver the same amount of energy as NG in today's pipelines. Higher concentrations allow for significantly greater energy delivery: for example, 15% A-A can deliver up to three times the energy of NG in a typical city gas network. At the upper end, a 47% concentration—the highest stable concentration for an A-A solution—could enable the current NG infrastructure to deliver up to nine times more energy than it does with NG today.

It is worth noting here that 15% concentration is comparable to that found in household cleaners, reinforcing its practicality and safe handling.

2.4. Fuel and water synergy

A unique aspect of the system is its ability to deliver both fuel and water to the power plant. Since thermal power plants consume large volumes of water for cooling and steam generation, transporting water with the fuel reduces dependency on local water sources. Depending on the A-A concentration, the water delivered with the fuel can fully meet the plant's operational needs. This makes A-A particularly attractive for inland or arid locations where water scarcity is a concern.

Moreover, the water extracted during ammonia separation is of high purity, approaching distilled quality. It can therefore be used directly in the steam cycle or for other industrial purposes with minimal treatment.

2.5. Storage and long-term availability

In evaluating alternatives to NG, storage conditions represent a critical consideration, as power plants generally require both short-term and long-term fuel storage systems to ensure a stable fuel supply and accommodate fluctuations in consumption.

Hydrogen requires high-pressure tanks or cryogenic systems, which are both expensive and energy-intensive. Pure ammonia must be stored at approximately 12 bar to remain liquid at ambient temperatures, and any loss of pressure risks a dangerous phase transition.

Storage of A-A is simpler and safer than that of either hydrogen or pure ammonia. A-A can be stored at atmospheric pressure, albeit in slightly larger volumes due to its lower energy density per unit mass. Still, the trade-off is acceptable given the improved safety profile and the elimination of costly pressurization infrastructure. For example, storing 1 TWh of energy in a 30% A-A would require approximately 2 times the volume of pure ammonia, but the associated storage infrastructure would be considerably more cost-effective and easier to maintain.

The use of A-A also presents an opportunity to decouple energy generation from real-time ammonia production. A-A can be synthesized in centralized facilities located away from populated areas, stored in atmospheric tanks, and then transported as needed. This flexibility enhances grid resilience and supports seasonal or diurnal load balancing in power generation.

3. Methodology

3.1. System description

The proposed concept is simple and practical: we suggest using A-A both as a fuel and as a medium for transporting water to power plants. The process begins with the off-site preparation of A-A, where ammonia is mixed with water in a controlled facility. This production site could be located near existing ammonia storage terminals or industrial ammonia sources, allowing for bulk processing and improved safety management away from urban areas.

The production unit consists of three storage tanks: one containing water, another containing ammonia, and a third for controlled mixing of the two streams. Non-potable water sources, such as harvested rainwater, may also be employed. Pressurized liquid ammonia (typically

around 12 bar) is supplied to the unit, where its pressure is regulated to match that of the water and transmission lines. The two flows are then combined in the required ratio to produce A-A. The ammonia gas is then blended with liquid water to form A-A at the desired concentration—typically between 10 and 15% by mass for heating applications, and 18–25% for power generation.

Once prepared, the A-A mixture is transported through the existing NG pipeline network to power plants. Upon arrival, the mixture enters a separation unit, where ammonia is thermally extracted for combustion—feeding a boiler system to generate steam. The remaining water can be reused within the plant—for instance, as feedwater—or distributed for industrial or municipal use. This dual-purpose transport of energy and water provides significant logistical and economic advantages, particularly for inland or arid regions where water availability is limited.

The extracted ammonia is combusted in a high-efficiency boiler, generating superheated steam that drives a double-extraction Rankine cycle. The system also functions as a combined heat and power (CHP) plant, utilizing residual heat from combustion and exhaust gases to support the A-A separation process and provide thermal energy to nearby facilities if required. Fig. 3 shows the total process from preparation to the power generation.

3.2. Thermodynamic modelling framework

To evaluate the viability of A-A as a power plant fuel, a rigorous thermodynamic model was developed using EES software. To accurately assess the performance of the new power generation system, we developed a detailed comprehensive thermodynamic model that incorporates the A-A production unit, transmission lines, and power plant systems, as illustrated in Fig. 3.

The model simulates the behaviour of a 200 MW steam power plant configured with a double-extraction Rankine cycle and two open feedwater heaters (FWHs). This cycle configuration enhances thermal efficiency by recovering more energy through staged feedwater heating, thereby reducing boiler heat input. The working cycle of this power plant is shown in Fig. 4-a. The key design parameters and operational conditions of the power plant are summarized in Table 1.

Table 1
Comparison of key performance parameters between the proposed steam cycle model and two real-world steam power plant case studies of Shahid Montazeri Power Plant and Khoms Steam Power Plant. Values are taken from [45].

Parameter	Present Model	Study A – Shahid Montazeri	Study B – Khoms Power Plant
Net Power Output (MW)	200.0	200.0	100.83
Boiler Pressure (bar)	160.0	130.0	128.0
Turbine Inlet Temperature (°C)	540	540	540
Condenser Pressure (kPa)	10	~10	~10
Steam Flow Rate (kg/s)	210.1	186.1 (670 T/h)	104.2 (375 T/h)
Fuel Type	Ammonia	NG	Heavy Fuel Oil (HFO)
Fuel Flow Rate (kg/s)	30.66	~15.5 (est. from 54 Nm^3/h)	25.34
Fuel Heating Value (kJ/kg)	18,600	48,806	44,514
Thermal Efficiency (%)	41.26	37.52	32.75
Overall (Net) Efficiency (%)	35.07	35.81 (7 FWHs) → 37.52 (9 FWHs)	32.16
No. of Feedwater Heaters (FWHs)	2	9	1 (proposed open-type)
Pump Efficiency (%)	85	95	–
Feedwater Temp into Boiler (°C)	254.0	247	–

Mass and energy balances were applied at each state point in the cycle using standard thermodynamic relationships. The specific enthalpies, entropies, mass fractions, and work/heat transfers were computed for each component. The model also accounts for combustion efficiency, heat losses, and auxiliary power consumption from pumps and other subsystems. One of the most critical components of the cycle is the ammonia-water separator. In this study, the location and method of supplying energy to the separator are thoroughly investigated.

NG, currently the primary fuel for the power plant, is used as a reference benchmark for comparison with the proposed A–A-based system. The behaviour of real gases often deviates from ideal gas assumptions due to interactions between molecules and the finite volume they occupy. To account for these deviations, the compressibility factor, Z is introduced, modifying the ideal gas law to:

$$PV = Z\,nRT \tag{2}$$

where, Z quantifies how much the gas departs from ideal gas and can be defined as the ratio of the actual volume to the ideal gas volume under the same conditions:

$$Z = \frac{V_{\text{real}}}{V_{\text{ideal}}} \tag{3}$$

For A-A, the fluid behaviour can often be approximated as an incompressible fluid. In contrast, for pure ammonia, NG, and hydrogen the behaviour depends on pressure, where it can exhibit both compressible and incompressible properties.

The model evaluates energy balances by calculating the mass flow of the transfer fluid and determining both the power generation capacity delivered to the power plant and the energy consumed by each component. Pure ammonia typically has an LHV of 18.8 MJ/kg, decreasing—for example—to 2.44 MJ/kg in a 13% A-A solution. Interestingly, A-A has a higher LHV per unit volume compared to pure ammonia and NG, especially under the pressures of current gas pipelines (see Fig. 1). This highlights the superior potential of A-A compared to pure ammonia and even hydrogen.

Fig. 5 illustrates the overall solution flowchart and the thermodynamic modelling framework of the system. In this framework, the power plant input data and operating conditions are first defined, followed by the modelling of the ammonia separation system from aqua-ammonia, ammonia combustion, and the power plant thermodynamic cycle. Subsequently, based on the power plant performance results, energy losses are evaluated and the appropriate energy supply location for the separation system is determined. Accordingly, the performance parameters of both the power plant and the separation system are updated in a coupled manner, accounting for their mutual interactions. The detailed modelling of each block shown in the flowchart is presented separately in the following sections.

3.2.1. A-A preparation

The ammonia storage unit (as shown in Fig. 3) uses insulated tanks, pressurizing ammonia to 12 bars to conserve space and maintain its liquid state. After passing through the expansion valve, ammonia pressure is adjusted for transmission. The fluid exiting the pressure-reducing valve is at a low temperature, absorbing heat from the ground or surrounding air via a heat exchanger to reach ambient temperature. The governing equations for the pressure-reducing valve or expander, and evaporator are as follows:

$$h_e = h_i \text{ (valve)} \tag{4}$$

$$\text{Or } W_e = h_i - h_e \text{ (expander)} \tag{5}$$

$$\dot{Q}_e = \dot{m}_{r1} h_e - \dot{m}_{r1} h_i \text{ (evaporator)} \tag{6}$$

The mixing tank in the AA production unit plays a crucial role in blending the two fluids, as described by the following equation:

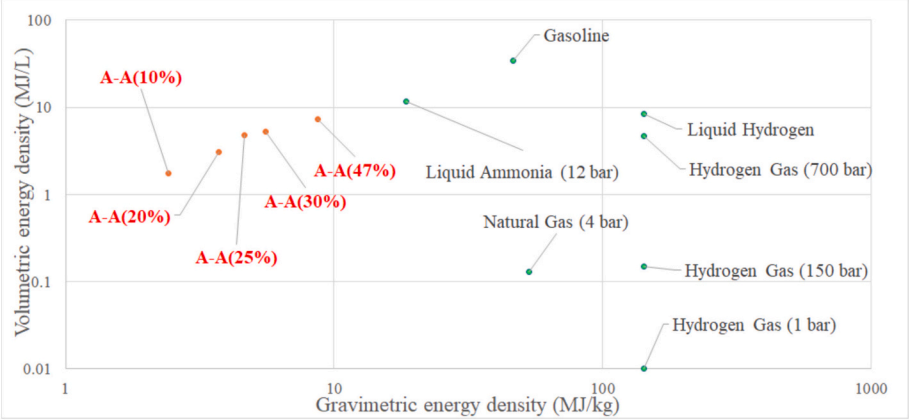

Fig. 1. The heating value of various fuels.

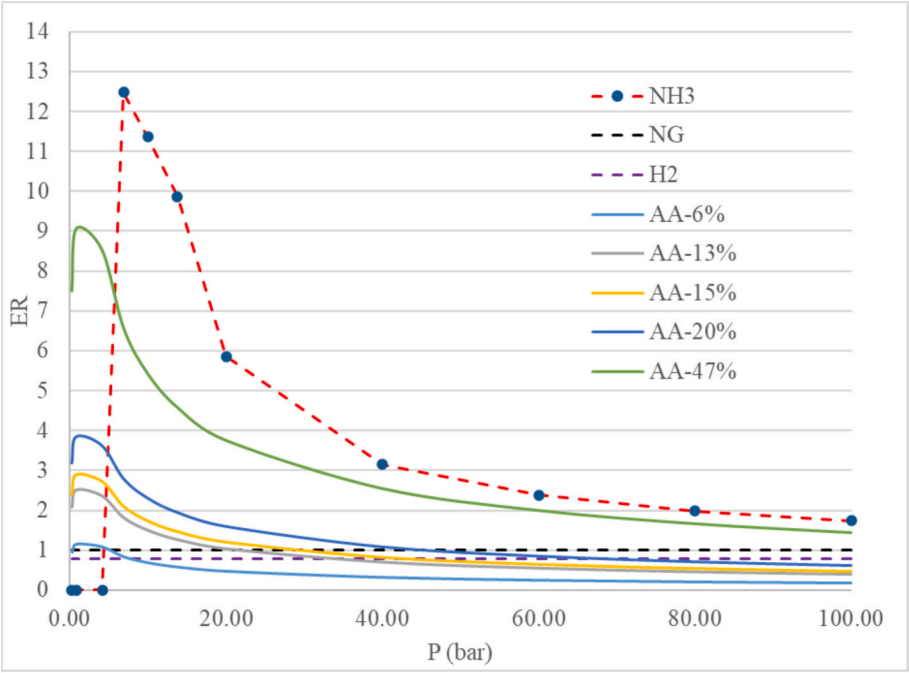

Fig. 2. Energy Ratio in pipelines with different pressures.

$$NH_3 + H2O \rightarrow NH_4OH$$

$$NH_4OH \rightarrow NH_4^+ + OH^- \quad (7)$$

The energy equation in the mixing tank is as follows:

$$\dot{m}_{r1} + \dot{m}_w = \dot{m}_p$$

$$\dot{Q}_{Cool} = \dot{m}_w h_2 + \dot{m}_{r1} h_1 - \dot{m}_p h_{e,3} \quad (8)$$

Mixing ammonia with water is an exothermic process that increases the temperature of the fluid. Although the released thermal energy could be harnessed for various applications, this paper emphasizes a worst-case scenario to provide a conservative estimate of energy dynamics. In this scenario, we assume that all generated heat is lost to the ground during transmission through the pipelines as follows:

$$\dot{Q}_e = \dot{m}_p h_4 - \dot{m}_p h_3 \quad (9)$$

3.2.2. Separation process

A critical addition to the traditional Rankine cycle configuration is the separation unit, which isolates ammonia from the incoming A-A mixture. Several methods are available for this separation, with complete evaporation being the least efficient. Three separation strategies, listed in Table 2 are comprehensively investigate in this study.

These methods differ in energy requirements, operating temperatures, and heat source suitability. The first method, that deals with complete evaporation of A-A mixture is known as the least efficient option. The model evaluates energy consumption of each method relative to the ammonia's heating value—referred to as the Separation Energy Ratio (SER). The impact of each separation approach on overall plant efficiency is analysed in subsequent sections. In this study, three potential sources for supplying energy to the separation unit are investigated: (1) the waste heat from the condenser, (2) the residual heat in the power plant stack, and (3) the heat exchange occurring in the plant's boiler. These three scenarios are illustrated in Fig. 4-b.

For the worst-case scenario of total fluid evaporation for the separation of water and ammonia. The governing equations for the evaporation tank are outlined below:

$$\dot{Q}_g = \dot{m}_{ex} h_8 - \dot{m}_{ex} h_7 \quad (10)$$

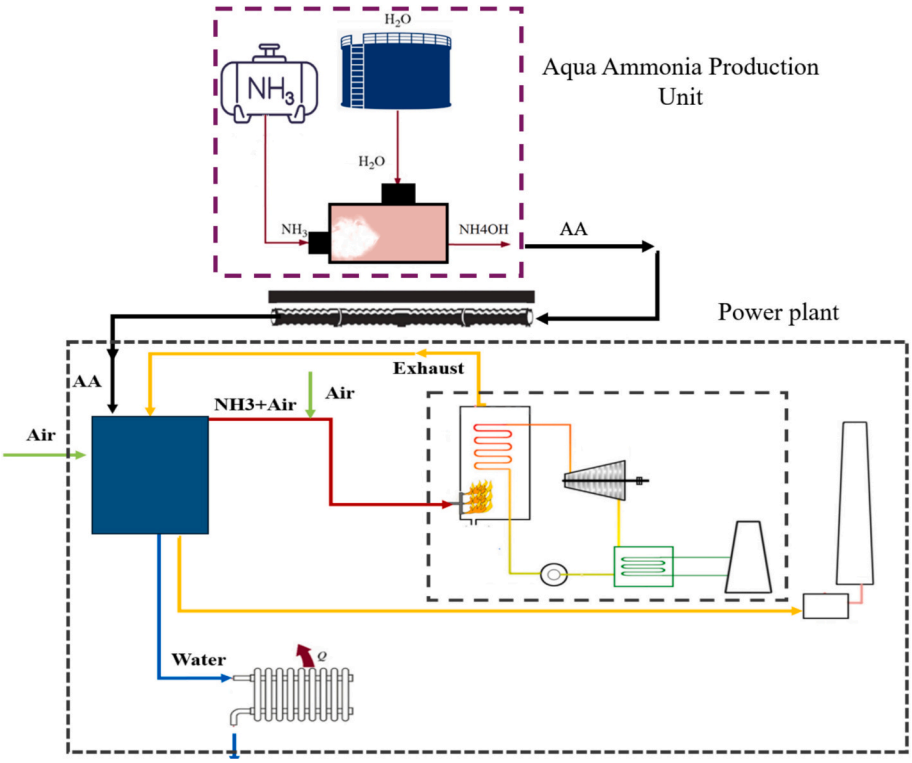

Fig. 3. Proposed cycle for steam power plant.

The separation tank can be modelled as follows:

$$\dot{Q}_g = \dot{m}_4 h_4 - \dot{m}_6 h_6 - \dot{m}_9 h_9 + \dot{m}_{air} h_{a,5} - \dot{m}_{air} h_{a,6} \tag{11}$$

Ammonia combustion takes place, releasing its internal energy, as depicted in the following equation:

$$4NH_{3(g)} + 3\left(O_{2(g)} + 3.75N_{2(g)}\right) \rightarrow 13.25N_{2(g)} + 6H_2O_{(g)} + Q$$

$$Q = H_{prod} - H_{react} \tag{12}$$

where,

$$H_{prod} = \sum N_p \left(\overrightarrow{h_f} + \overline{h} - \overline{h}^{\circ}\right)_p \tag{13}$$

$$H_{react} = \sum N_r \left(\overrightarrow{h_f} + \overline{h} - \overline{h}^{\circ}\right)_r \tag{14}$$

The exhaust from the ammonia combustion burner contains water vapor, along with nitrogen and probably NOx at high combustion temperatures.

3.2.3. Steam power plant

The power cycle follows fundamental thermodynamic principles based on the first and second laws of thermodynamics. Steam is generated in the boiler, expanded through a multi-stage turbine, with intermediate extractions to feedwater heaters, and finally condensed. The modelling framework ensures the conservation of energy and mass across all cycle components. Thermodynamic modelling was carried out to evaluate its performance using ammonia—previously extracted from the A-A solution—as the combustion fuel.

The power cycle consists of the following key components:

- A high-pressure boiler producing superheated steam at 16 MPa and 540 °C.
- A multi-stage turbine with three steam extraction points: 4 MPa, 0.7 MPa and 0.01 MPa.
- Two open feedwater heaters (FWHs) that preheat the boiler feedwater by recovering thermal energy from steam extracted at two stages: the high-pressure extraction point (FWH2) and the low-pressure extraction point (FWH1).
- A condenser operating at 10 kPa.
- Three pumps: two associated with the FWHs and one main boiler feed pump.

Turbine, pump and boiler isentropic efficiencies are assumed 88%, 85% and 85% respectively.

Each component has its own energy balance, which must be integrated with the governing thermodynamic relations to obtain a complete system model. The corresponding equations for each element are presented below.

Energy balance for FWHs

$$(1 - y_2 - y_1)h_{17} + y_2 h_{14} = (1 - y_1)h_{18} \tag{15}$$

$$(1 - y_1)h_{19} + y_1 h_{13} = h_{20} \tag{16}$$

Turbine work output

$$W_{turbine} = W_{12\rightarrow13} + (1 - y_1)W_{13\rightarrow21} + (1 - y_2)W_{21\rightarrow14} + (1 - y_2 - y_1)W_{14\rightarrow15} \tag{17}$$

Pumps work input

$$W_{Pumps} = (1 - y_2 - y_1)W_{Pump1} + (1 - y_2)W_{Pump2} + W_{Pump3} \tag{18}$$

Boiler heat input

$$Q_{Boiler} = h_{11} - h_{12} \tag{19}$$

Condenser heat rejection

$$Q_{Condenser} = (1 - y_2 - y_1)h_{710} - h_1 \tag{20}$$

Eqs. (4)–(20) collectively describe the system from A-A preparation through to power generation. The following section evaluates the model's performance.

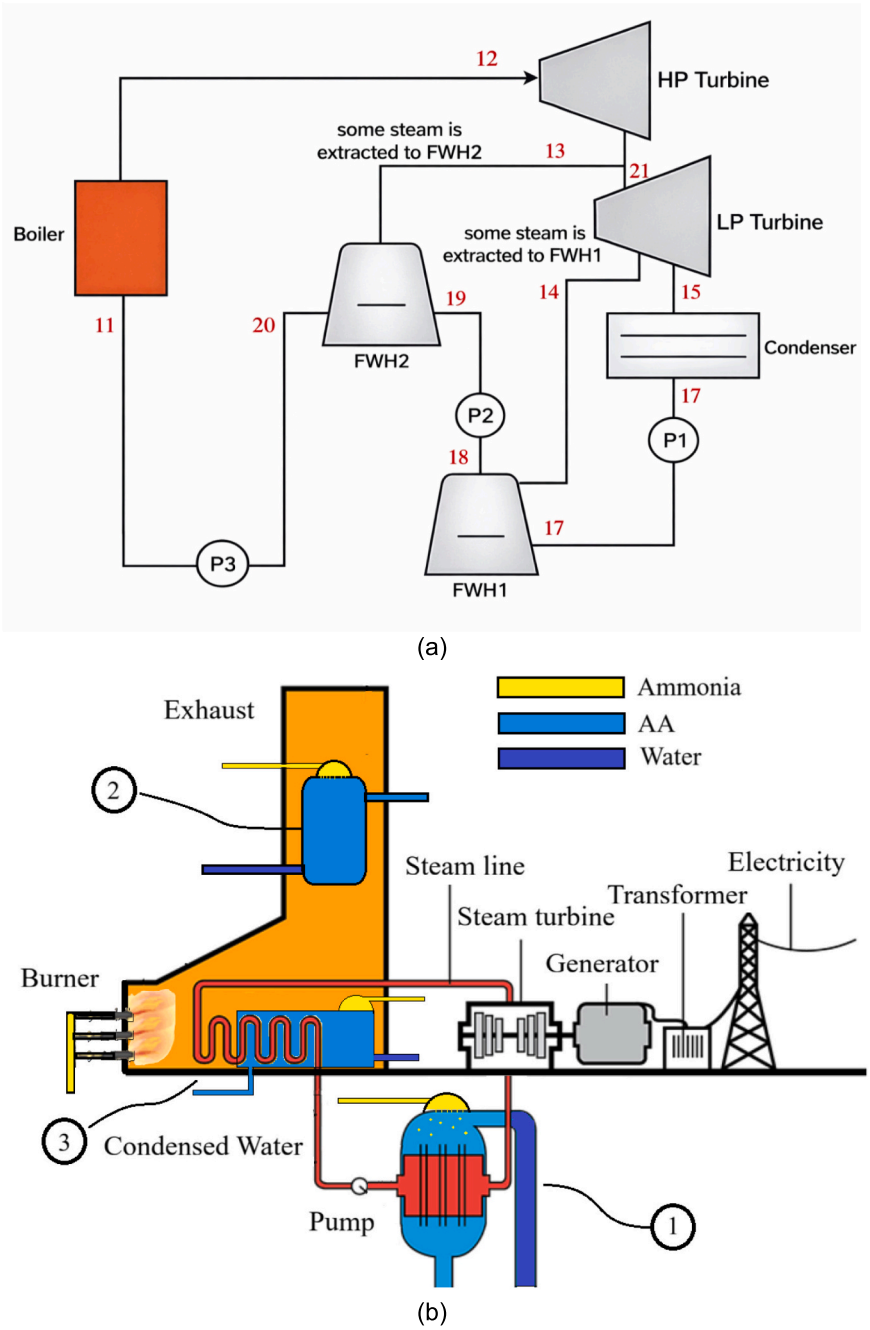

Fig. 4. Schematic of the considered steam power generation cycle. (a) The modelled cycle. (b) Locations where the ammonia separator system from A-A can be installed.

4. Validation

To validate the proposed steam cycle model, a comparative analysis was conducted against two real-world case studies documented in peer-reviewed literature [45,46]. Table 1 summarizes the main thermodynamic and operational parameters. The Shahid Montazeri power plant [32], with a net output of 200 MW, uses nine FWHs and achieves thermal and exergy efficiencies of 37.52% and 41.7%, respectively [45] (Mohammed et al., 2019). The Khoms plant, operating at approximately 100 MW, achieves 32.75% thermal efficiency under its base configuration [46] (Ibrahim et al., 2011).

In Fig. 6, a comparison of the modelling results with the reference results [45] for natural gas fuel is presented. The good agreement between the results indicates the appropriate accuracy of the modelling.

Since in the proposed system, only the fuel is changed and the heat losses from the power plant are utilized in the separation system to produce ammonia from aqua-ammonia, and these changes do not significantly affect the power cycle itself (particularly its operating conditions), this validation is also applicable and valid for the power plant operating with ammonia fuel (or, in other words, aqua-ammonia).

In this article, to focus primarily on the power plant performance due to the fuel change and to better utilize the heat losses from the condenser and boiler in the proposed cycle, a simpler cycle (with only 2 feedwater heaters) and different operating conditions compared to the actual cycle of the Shahid Montazeri power plant has been used. This cycle, in comparison with reference [45], has higher boiler pressure and greater steam mass flow rate, making it more suitable for this investigation while also exhibiting better performance than the cycles used for

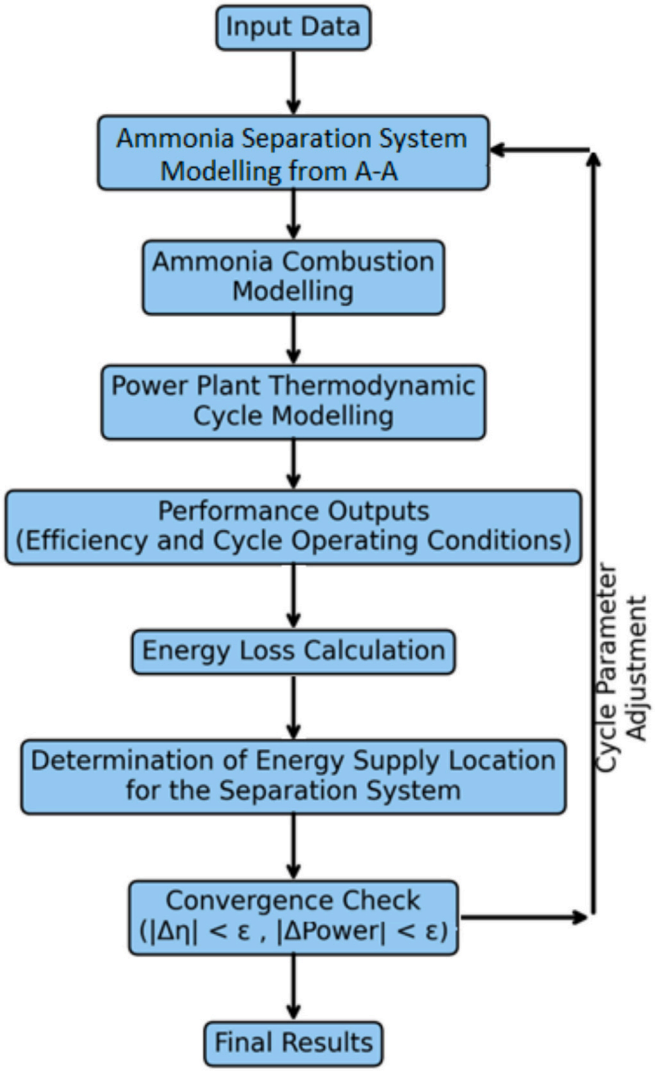

Fig. 5. Flowchart of the integrated thermodynamic modelling framework.

validation.

The full specifications of this cycle are provided in Table 1, and its efficiency results for ammonia fuel are shown in Fig. 6 as a function of different boiler pressures.

Compared to these facilities, the current model operates at a boiler pressure of 16 MPa and demonstrates superior thermal (41.26%) and net (35.07%) efficiencies with only two feedwater heaters. These results confirm the thermodynamic advantage of the model, especially in terms of energy utilisation and reduced complexity. The higher efficiency can be attributed to optimal mass flow design and turbine performance assumptions within the ammonia-fuelled cycle framework.

In the subsequent sections, the topic of energy losses due to the separation of ammonia from aqua-ammonia will be discussed in detail. However, even in the simplest case—where the energy required for separation is supplied from the power plant's heat losses—the performance penalty resulting from switching the fuel from pure ammonia to aqua-ammonia is also shown in Fig. 6. This penalty is relatively minor and, compared to the significant advantages offered by this approach, appears highly promising.

5. Results and discussion

5.1. Base cycle performance

The baseline configuration of the modelled steam power plant utilizes A-A as a transport medium and ammonia as the combustion fuel. After modelling, two key components, namely the separation unit and the power plant using ammonia as fuel, have been simulated. To this end, the power plant depicted in Fig. 4-a, which operates with ammonia fuel, has been modelled. The Rankine cycle was modelled with a boiler pressure of 16 MPa and a superheated steam temperature of 540 °C. The condenser operated at 10 kPa, and steam was extracted at 4 MPa and 0.7 MPa for feedwater heating. The cycle delivered a net output of 200 MW with a gross thermal efficiency of 41.26% and net thermal efficiency of 35.07%, as shown in Table 3. Table 3 presents the base-case energy and mass balances for the 200 MW Rankine cycle. Two points are especially important: (1) the gross thermal efficiency of 41.26% is achieved with only two open FWHs — showing the effectiveness of the chosen extraction pressures — and (2) the fuel mass flow (30.66 kg s^{-1} of ammonia) together with boiler heat input (~485 MW**) establish the scale of separation and fuel-supply infrastructure required. These values set the baseline for sensitivity studies and demonstrate that ammonia from A-A can meet utility-scale loads with acceptable cycle performance.

The calculated ammonia fuel flow rate was 30.66 kg/s (ammonia), and the feedwater reached 254 °C at boiler inlet. These results reflect the high regenerative effectiveness achieved with only two open FWHs and validate the overall design for mid-scale generation. Table 4 investigates the impact of increasing LP FWH extraction pressure. Although regenerative heating improves due to higher extraction at the LP stage, efficiency declines slightly (from 41.45% to 41.03%) as available energy for turbine expansion is reduced. This highlights a trade-off between feedwater preheating and mechanical energy extraction, especially in the low-pressure turbine stages. Similarly, Table 5 examines the effect of high-pressure extraction pressure. It shows an optimal region around ~4000 kPa HP extraction where regenerative benefits and turbine enthalpy drop are balanced. Beyond ~4000 kPa the gross efficiency declines. The efficiency penalty (dropping to 40.20% at 8000 kPa) demonstrates the existence of an optimum around 4000 kPa, beyond which the regenerative gains are offset by losses in expansion work. The results here justify the chosen HP extraction point in the base case and highlight that HP extraction should be tuned alongside turbine stage design to avoid efficiency penalties. While increased extraction improves feedwater heating, it results in reduced turbine enthalpy drop and higher pump work. The influence of boiler pressure, reported in Table 6. Table 6 demonstrates classical Rankine behaviour: increasing boiler pressure raises gross efficiency from 39.33% at 10 MPa to 42.02% at 20 MPa, due to increased turbine enthalpy drop. However, the rate of improvement diminishes beyond 19,000 kPa, indicating thermodynamic saturation and increased pump work. This validates conventional boiler pressure limits in utility-scale designs. Practically, material limits and economics often constrain designs below the maximum thermodynamic optimum; thus, the table provides both the theoretical trend and a reminder to consider metallurgical and cost constraints when selecting boiler pressure. In Fig. 7, the effect of boiler pressure on the overall performance of the power plant is shown. The plot shows an initially steep efficiency increase with pressure that then flattens beyond ~18 MPa. This behaviour indicates diminishing thermodynamic returns for very high pressures and supports a design choice that balances achievable efficiency gains with boiler metallurgy and capital costs. Table 7 quantifies how lowering condenser pressure increases gross thermal efficiency (up to 42.78% at 5 kPa) by enlarging the turbine expansion ratio. However, pressures below ~8 kPa introduce practical challenges such as larger condenser size and more demanding vacuum systems, limiting feasibility in commercial applications. This table therefore highlights a performance–practicality trade-off: the highest efficiencies

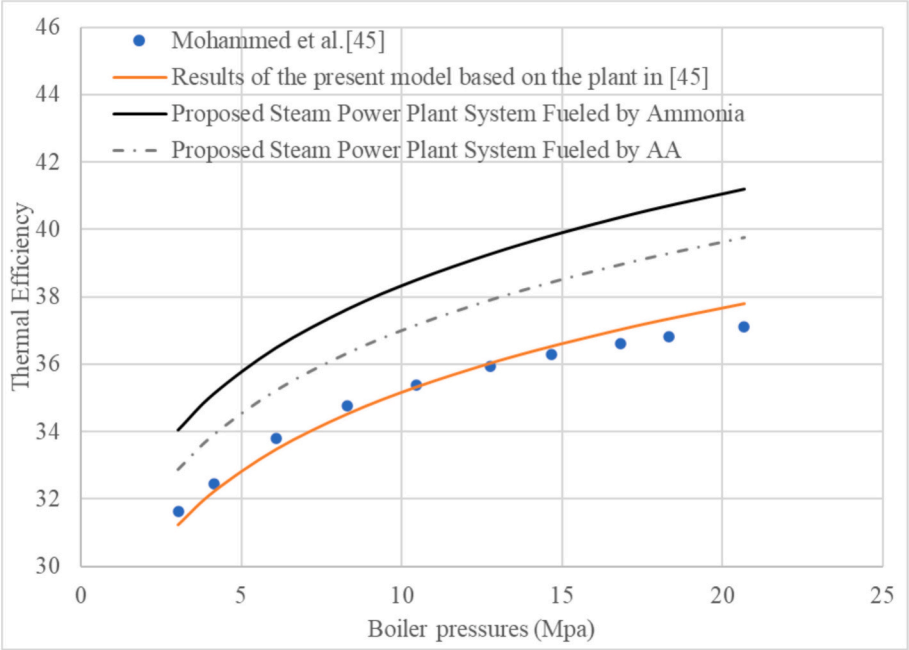

Fig. 6. Validation of the numerical model against Ref. [45] for natural gas, and net efficiency of the proposed cycle with pure ammonia and aqua-ammonia fuels versus boiler pressure. (For interpretation of the references to colour in this figure legend, the reader is referred to the web version of this article.)

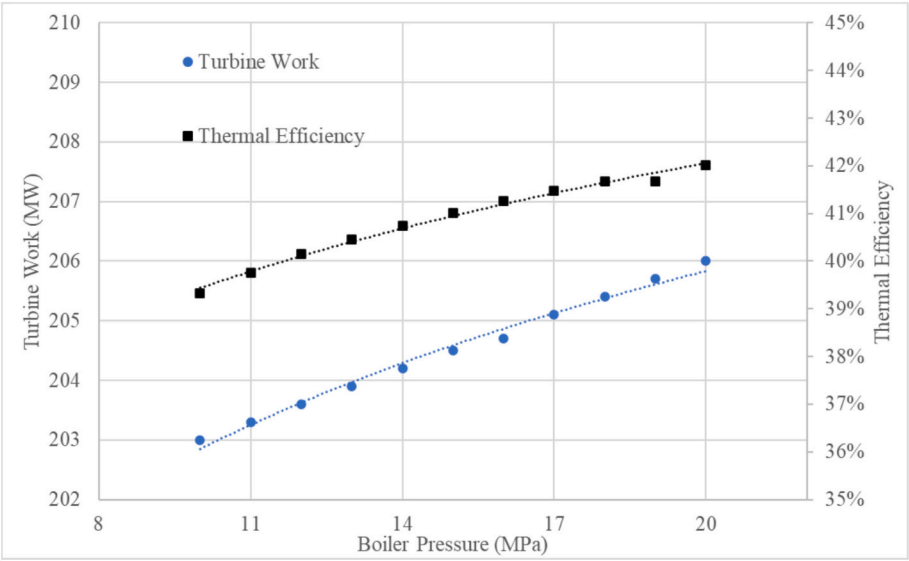

Fig. 7. Effects of boiler pressure in thermal efficiency and the turbine work.

require substantial balance-of-plant investments and may not be optimal for retrofit projects where capital and footprint are constrained. Table 8 shows that increasing boiler outlet temperature from 480 °C to 600 °C improves efficiency by over 2 percentage points and reduces fuel consumption by 5%. These gains are achieved without altering turbine or extraction configuration. However, temperatures beyond 600 °C would require advanced materials due to metallurgical constraints, limiting further optimisation. Therefore, temperature increase is an effective lever for efficiency but has trade-offs with materials and lifecycle maintenance costs. Table 9 demonstrates that off-design operation (80–200 MW) maintains nearly constant extraction fractions, confirming the flexibility of the regenerative configuration. Steam flow and heat recovery scale linearly at higher loads; however, below ~70% capacity, effective control of extraction and feedwater heating becomes essential to prevent efficiency losses and operational imbalance. Tables 9 and 10 highlight the role of component efficiencies. Table 10 shows turbine performance is a dominant driver of overall plant efficiency: improving isentropic turbine efficiency from 0.80 to 0.90 increases gross efficiency from **38.2% to 42.01%** and reduces fuel flow by ~9%. This highlights that technology choices for the turbine (stage design, inlet conditions, blade cooling) are principal enablers for realising A-A system benefits. Investment in high-efficiency turbine stages yields outsized returns compared to marginal pump improvements. Pump efficiency improvements show smaller gains but are critical in reducing auxiliary losses, particularly in high-pressure systems. Both underscore the importance of component-level optimisation in achieving high net output without compromising system integrity.

Table 11 indicates that pump efficiency primarily affects auxiliary

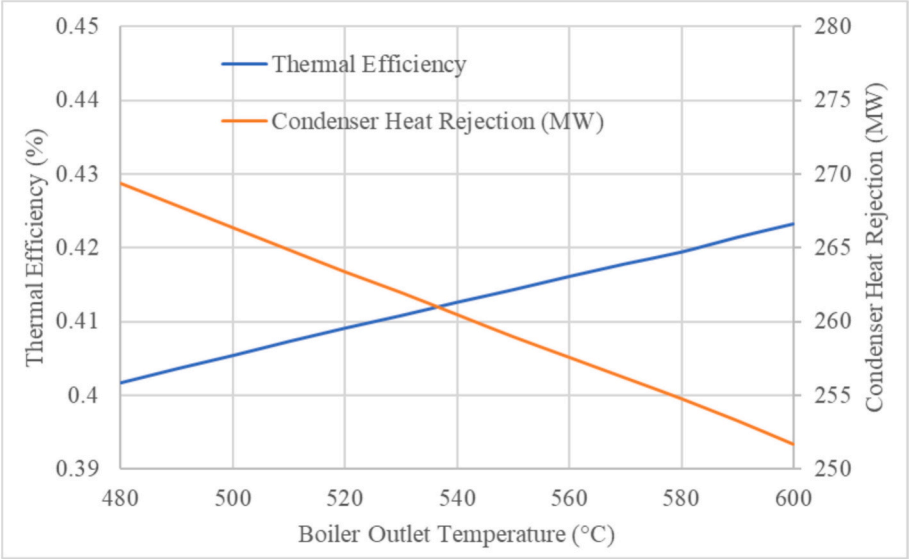

Fig. 8. Condenser heat losses and efficiency as a function of boiler outlet temperature.

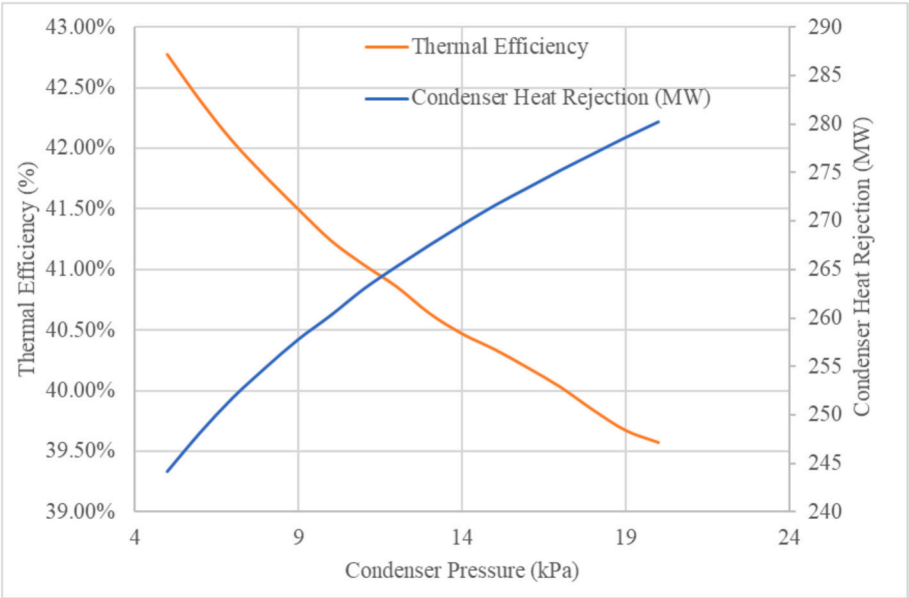

Fig. 9. Condenser heat losses and efficiency as a function of condenser pressure.

power rather than core turbine output: improving pump efficiency from 0.7 to 0.9 reduces pump work from 5.82 MW to 4.499 MW. Although the absolute change is modest compared to turbine gains, high pump efficiency contributes materially to net plant output in high-pressure cycles and should not be neglected when seeking incremental gains in net efficiency.

One of the most important results is the identification of significant heat losses, particularly in the condenser, which can be utilized in the ammonia separation system. Figs. 8 and 9 illustrate the condenser heat losses and the overall power plant efficiency as functions of parameters such as condenser pressure and boiler outlet temperature.

5.2. Impact of separation unit on system performance

The most significant modification in the power plant cycle, compared to conventional gas or ammonia-fired power plants, is the addition of a section dedicated to the separation of ammonia from water. Depending on the chosen separation method, a certain amount of energy is required in this process to ultimately obtain purified ammonia and water.

This study seeks to answer two fundamental questions: First, where in the power cycle is the most suitable location to supply the energy required for the separation unit? Second, which separation method is more technically and operationally appropriate for the power plant? Additionally, the study evaluates how integrating this separation system affects the overall performance of the power plant, particularly its efficiency. Three separation methods (Evaporative separation, Ammonia Boiling-based and Membrane-based separation) have been considered as the basis for modelling in this study.

The key differences among these three methods lie in their operating temperatures and the energy required for separation. To supply the energy demand of the separation unit, two main strategies are proposed:

- First scheme: Utilizing waste heat from the power plant

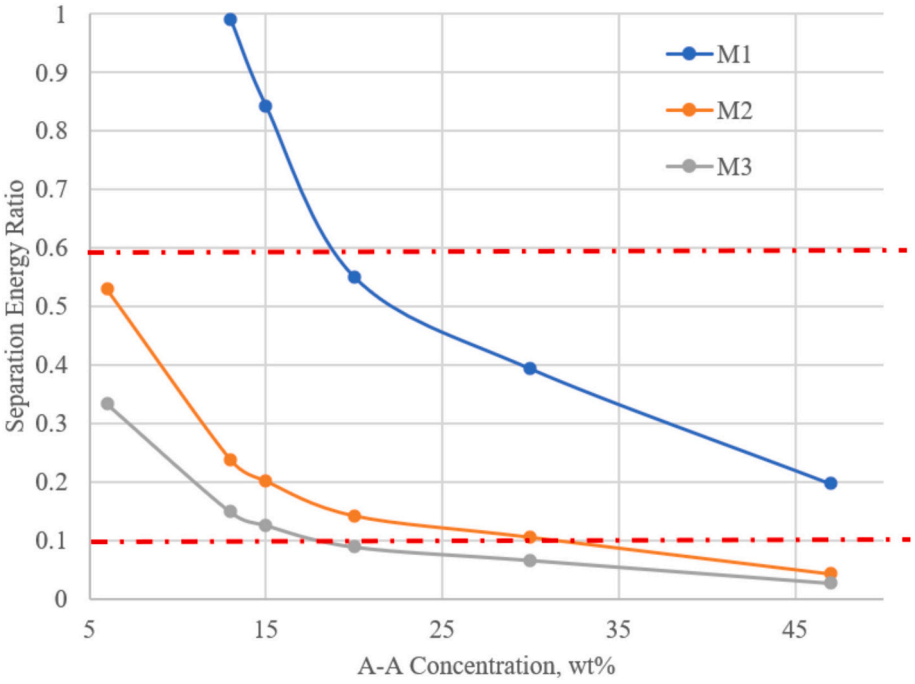

Fig. 10. SER for different ammonia-water separation methods.

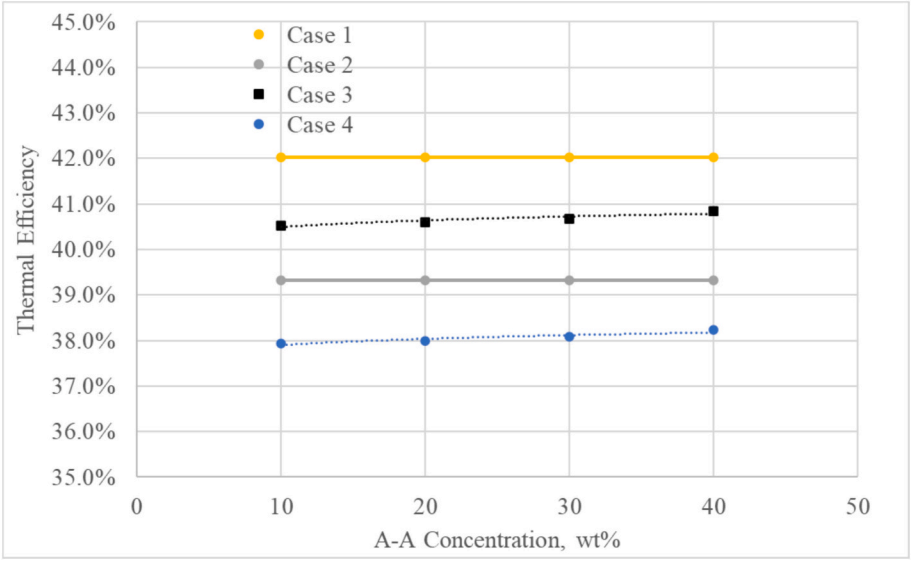

Fig. 11. Impact of separation strategy and condenser pressure on overall plant efficiency.

- Second scheme: Directly use a portion of fuel to cover this

It is worth noting that the chemical energy required for separating ammonia from water, or breaking the molecular bonds, is approximately 2.5% to 3.5% of the fuel's heating value [34]. This portion represents an inherent energy loss that cannot be recovered by any other means. However, when evaluated at the scale of the entire power plant, the actual impact of this separation process on overall efficiency is less than 1%. This effect has been thoroughly examined and quantified in this study.

5.2.1. First scheme: utilizing waste heat from the power plant to provide energy for separation

In gas turbine power plants, the exhaust gases have high temperatures and significant energy content, making the use of exhaust heat for the separation process both straightforward and feasible. In contrast, in steam power plants, most thermal losses occur in the condenser, where the temperature is relatively low. Theoretically, in a steam power plant, the temperature of the flue gases exiting the boiler stack is only slightly higher than the temperature of the water entering the boiler. This implies that stack losses are minimal compared to condenser losses. However, in practice, only about 5% to 10% of the fuel's heating value remains in the exhaust gases.

To determine the appropriate heat source for the separation process, it is essential to evaluate how much of the fuel's heating value must be allocated for this purpose. For this, a parameter called the Separation Energy Ratio (SER) is defined, representing the ratio of the energy consumed in the separator to the total heating value of the fuel:

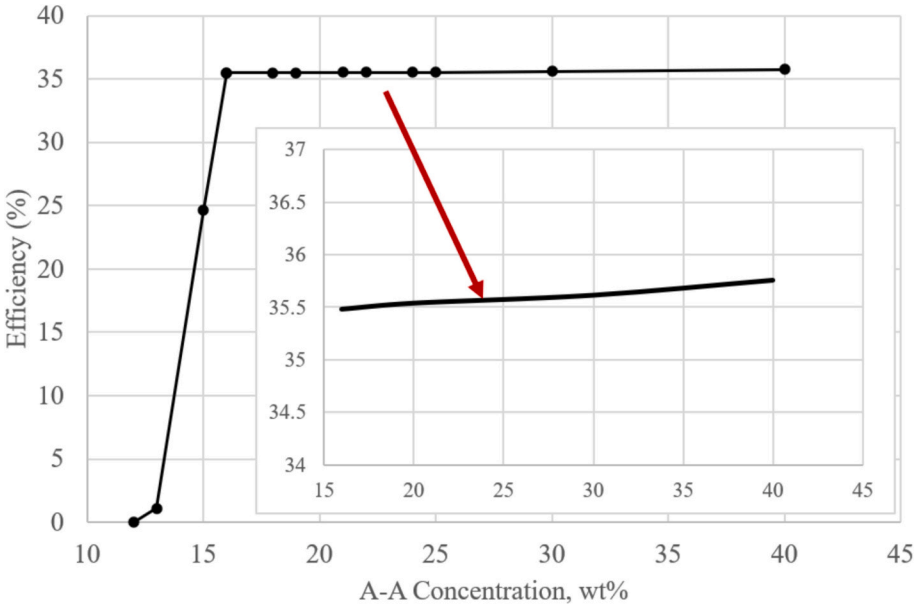

Fig. 12. Thermal efficiency of the power plant at different A-A concentrations, considering the energy limitation for complete ammonia separation using evaporative method with the separator located in the condenser.

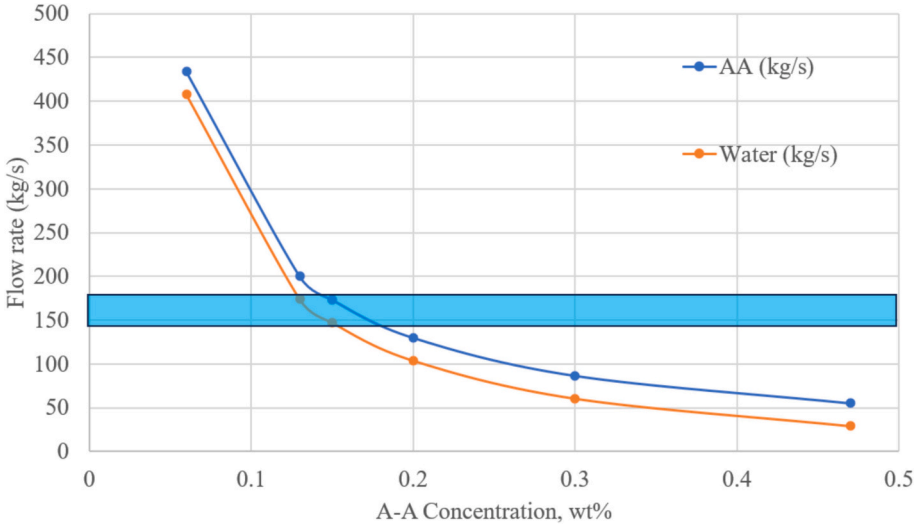

Fig. 13. Water supplied with A-A compared to power plant cooling requirements.

Table 2
Separation methods considered comprehensively in this study.

Separation Method	Description
M1	Evaporative separation that relies on complete evaporation of the A-A mixture
M2	Ammonia Boiling-based separation where water remains in a saturated liquid state
M3	Membrane-based separation, with fluid maintained at a temperature between ambient and boiling point

$$\text{SER} = (\text{Energy used in the separation unit})/(\text{Fuel's heating value}) \tag{21}$$

Fig. 10 presents this parameter for the three separation methods shown as M1, M2 and M3. On the other hand, according to the obtained results the thermal efficiency of the cycle ranges between 39% and 43%, meaning that, on average, around 59% of the fuel's energy is lost through the condenser and boiler stack. In Fig. 10, this 59% value—along with an estimated 10% potential loss in the exhaust—is marked with a red line. This diagram plays a key role in evaluating and selecting the separation method, the input concentration of A-A to the power plant, and the appropriate heat source (either exhaust or condenser). It helps determine whether the available energy at a given point is sufficient to meet the separation process requirements.

In addition to the quantity of available energy, its quality—defined by temperature—is a critical consideration. Exhaust heat represents high-grade thermal energy due to its elevated temperature, but it is typically available in limited quantities. In contrast, condenser waste heat is more abundant but constitutes low-grade heat because of its lower temperature. Therefore, selecting an appropriate separation method requires careful consideration of both the quantity and grade (quality) of the available thermal energy.

If the design is based on using waste heat from the condenser, we would deal with temperatures range between 32 °C (corresponding to 5

Table 3
Performance summary of the base-case Rankine cycle.

Parameter	Value
Boiler Pressure	16 MPa
High-Pressure Extraction	4 MPa
Low-Pressure Extraction	0.7 MPa
Condenser Pressure	0.01 MPa
Boiler Outlet Temperature	540 °C
Net Power Output	200 MW
Mass Flow Rate	210.1 kg/s
Condenser Mass Flow Rate	131.3 kg/s
Fuel Mass Flow Rate	30.66 kg/s
Extraction Fraction at FWH1	0.2112
Extraction Fraction at FWH2	0.1637
Boiler Heat Input	484.7 MW
Condenser Heat Rejection	260.5 MW
FWH1 Heat Transfer	90.21 MW
FWH2 Heat Transfer	67.84 MW
Turbine Total Work	204.8 MW
Total Pump Work	4.77 MW
Gross Thermal Efficiency	41.26%
Net Thermal Efficiency	35.07%

kPa) and 60 °C (corresponding to 20 kPa), as shown in Table 7. Within this range, the membrane-based method (M3) appears to be the most suitable. Moreover, increasing the condenser pressure raises the temperature of the waste heat, which not only improves membrane separation performance but also makes other separation methods feasible.

Fig. 11 compares the thermal efficiency of the plant across four cases listed and described in Table 12.

Cases 1 and 2 represent Scheme 1, while Cases 3 and 4 correspond to the second scheme, which will be discussed in the next section. To evaluate how condenser operating conditions affect plant efficiency, two scenarios are considered: Case 1,3 with a condenser pressure of 5 kPa and Case 2,4 with 20 kPa. The results indicate that increasing the condenser pressure causes a drop in efficiency of about 3%, from 42.78% to 39.57%.

Fig. 11 shows that using boiler heat (cases 3–4) reduces dependency on condenser temperature and generally yields higher effective separation for a given A-A concentration, at the cost of a small direct fuel penalty (≈1–1.5%). Conversely, relying on condenser heat (cases 1–2) is only feasible with membrane separation or sufficiently high A-A concentrations.

If the goal is to use the boiling-based separation method (M1) with energy from the condenser, the simplest option would be increasing condenser pressure to 100 kPa, raising its temperature to around 100 °C. Table 13 quantifies the dramatic penalty of raising condenser temperature to 100 °C (100 kPa): net efficiency drops to ~29.5%, fuel flow rises substantially (36.43 kg s^{-1}), and condenser heat rejection increases markedly. These metrics demonstrate that coupling full evaporative separation to low-grade condenser heat is not viable for high-efficiency operation. Table 13 thereby justifies the focus on membrane-based separation or locating the separator in higher-grade heat locations (e.g., boiler) to avoid major efficiency losses.

This significant efficiency drop indicates that using the condenser in combination with the first separation method (i.e., full evaporative

Table 4
Impact of low-pressure FWH extraction pressure on cycle performance.

Low-pressure heater extraction pressure (kPa)	Low-pressure heater extraction fraction	High-pressure heater extraction fraction	Total mass flow rate (kg/s)	Total pump work (MW)	Total boiler heat input (MW)	Total condenser heat rejection (MW)	Gross thermal efficiency
400	0.1836	0.1951	209.2	4.734	482.5	257.6	41.45%
600	0.2034	0.173	209.8	4.759	484.0	259.5	41.32%
800	0.2181	0.1552	210.4	4.779	485.4	261.6	41.21%
1000	0.2298	0.1399	210.9	4.795	486.5	263.8	41.11%
1200	0.2397	0.1264	211.3	4.806	487.5	266	41.03%

Table 5
Impact of high-pressure FWH extraction pressure on cycle performance.

High-pressure heater extraction pressure (kPa)	Low-pressure heater extraction fraction	High-pressure heater extraction fraction	Mass flow rate (kg/s)	Total pump work (MW)	Boiler heat input (MW)	Condenser heat rejection (MW)	Gross thermal efficiency
2000	0.2058	0.09444	194.5	4.734	483.1	270.2	41.40%
3000	0.2058	0.141	202.5	4.421	483	264	41.40%
4000	0.2112	0.1637	210.1	4.77	484.7	260.5	41.26%
5000	0.2145	0.1878	217.4	4.994	487.3	258.5	41.05%
6000	0.2145	0.2083	224.6	5.199	490.3	257.3	40.79%
7000	0.2158	0.2264	231.8	5.387	493.8	256.7	40.51%
8000	0.217	0.2427	238.9	5.56	497.5	256.4	40.20%

Table 6
Effect of boiler pressure on performance.

Boiler pressure (kPa)	Steam extraction fraction y1	Steam extraction fraction y2	Total turbine work (MW)	Total pump work (MW)	Total boiler heat input (MW)	Total condenser heat rejection (MW)	Gross thermal efficiency
10,000	0.2012	0.1533	203	2.976	508.5	285.5	39.33%
11,000	0.2031	0.1553	203.3	3.271	503.1	279.9	39.75%
12,000	0.2049	0.1571	203.6	3.567	498.5	275.1	40.15%
13,000	0.2065	0.1589	203.9	3.865	494.4	270.9	40.45%
14,000	0.2082	0.1606	204.2	4.164	490.8	267.1	40.75%
15,000	0.2097	0.1622	204.5	4.465	487.6	263.6	41.02%
16,000	0.2113	0.1638	204.7	4.77	484.7	260.4	41.26%
17,000	0.2127	0.1652	205.1	5.077	482.2	257.7	41.48%
18,000	0.2141	0.1667	205.4	5.388	479.9	255.2	41.68%
19,000	0.2155	0.1681	205.7	5.702	477.8	252.9	41.68%
20,000	0.2169	0.1695	206	6.019	476	250.9	42.02%

Table 7
Effect of condenser pressure on thermodynamic performance.

Condenser pressure (kPa)	Low-pressure heater extraction fraction	Total pump work (MW)	Total boiler heat input (MW)	Total condenser heat rejection (MW)	Gross thermal efficiency
5	0.2243	4.601	467.5	244.2	42.78%
6	0.221	4.643	471.7	248.2	42.40%
7	0.2182	4.679	475.5	251.8	42.06%
8	0.2156	4.712	478.8	254.9	41.77%
9	0.2133	4.742	481.9	257.8	41.50%
10	0.2112	4.777	484.7	260.3	41.24%
11	0.2093	4.795	487.3	263	41.04%
12	0.2075	4.819	489.8	265.3	40.86%
13	0.2058	4.842	492.1	267.5	40.64%
14	0.2042	4.863	494.3	269.6	40.47%
15	0.2027	4.883	496.3	271.6	40.34%
16	0.2013	4.903	498.3	273.4	40.19%
17	0.1999	4.921	500.2	275.2	40.03%
18	0.1986	4.939	502	276.9	39.84%
19	0.1974	4.956	503.7	278.6	39.67%
20	0.1962	4.972	505.4	280.2	39.57%

Table 8
Effect of boiler outlet temperature on thermodynamic performance.

Boiler outlet temperature (°C)	Gross thermal efficiency	Fuel mass flow rate (kg/s)	Total condenser heat rejection (MW)
480	0.4017	31.49	269.4
490	0.4036	31.34	267.9
500	0.4054	31.2	266.4
510	0.4073	31.06	264.9
520	0.4091	30.92	263.4
530	0.4108	30.79	262
540	0.4126	30.65	260.5
550	0.4143	30.52	259
560	0.4161	30.4	257.6
570	0.4178	30.27	256.2
580	0.4194	30.15	254.8
590	0.4214	30.02	253.3
600	0.4232	29.89	251.7

Table 9
Effect of part-load (off-design) operation on feedwater heater performance.

Net power output (MW)	Total mass flow rate (kg/s)	Total heat transfer in low-pressure feedwater heater (MW)	Total heat transfer in high-pressure feedwater heater (MW)
80	84.04	36.08	27.13
90	94.54	40.6	30.53
100	105	45.11	33.92
110	115.6	49.62	37.31
120	126.1	54.13	40.7
130	136.6	58.64	44.13
140	147.3	63.14	47.49
150	157.6	67.63	50.88
160	168.1	72.17	54.27
170	178.6	76.68	57.68
180	189.1	81.19	61.08
190	199.6	85.7	64.48
200	210.1	90.21	67.84

Table 10
Effect of turbine efficiency on thermodynamic performance.

Turbine efficiency	Gross thermal efficiency	Fuel mass flow rate (kg/s)	Low-pressure heater extraction fraction (y1)	High-pressure heater extraction fraction (y2)
0.8	0.382	33.12	0.2066	0.1615
0.81	0.3859	32.79	0.2072	0.1618
0.82	0.3897	32.46	0.2077	0.1621
0.83	0.3936	32.14	0.2083	0.1623
0.84	0.3974	31.83	0.2089	0.1629
0.85	0.4013	31.53	0.2095	0.1629
0.86	0.4051	31.23	0.2102	0.1632
0.87	0.4089	30.94	0.2108	0.1634
0.88	0.4126	30.66	0.2112	0.1637
0.89	0.4164	30.38	0.2116	0.164
0.9	0.4201	30.11	0.2124	0.1643

Table 11
Effect of pump efficiency on auxiliary power consumption.

Pump efficiency	Total pump work (MW)	Total turbine work (MW)
0.7	5.82	205.8
0.72	5.654	205.7
0.74	5.497	205.5
0.76	5.349	205.3
0.78	5.208	205.2
0.8	5.075	205.1
0.82	4.948	204.9
0.84	4.828	204.8
0.86	4.713	204.7
0.88	4.604	204.6
0.9	4.499	204.5

Table 12
Four different cases considered for supplying the separation energy.

Scheme	Case	Description
Scheme 1: Utilizing waste heat from the power plant	Case 1	The power plant operates at a condenser pressure of 5 kPa, and the separation energy is supplied from the condenser
	Case 2	The power plant operates at a condenser pressure of 20 kPa, and the separation energy is supplied from the condenser
Scheme 2: Directly use a portion of fuel to cover this	Case 3	The power plant operates at a condenser pressure of 5 kPa, and the separation energy is supplied from the boiler
	Case 4	The power plant operates at a condenser pressure of 20 kPa, and the separation energy is supplied from the boiler

separation) is not an optimal choice. In contrast, the membrane-based separation method, which operates at lower temperatures, appears to be a more suitable alternative. Additionally, the A-A fluid itself plays an active role in the cooling process.

In power plants where the condenser operates at higher temperatures and the cooling fluid undergoes partial evaporation, the second method—complete evaporation of ammonia and partial evaporation of water—can be considered a viable design basis. In this approach, the A-A solution entering the condenser not only provides cooling but also facilitates the full evaporation of ammonia and partial evaporation of water. It is important to note that in A-A mixtures, depending on the concentration (e.g., 13%), the boiling point of the solution is significantly lower than that of pure water. As a result, ammonia begins to evaporate first and separates from the mixture.

This behaviour offers two key advantages: first, more effective cooling due to the refrigerant-like properties and lower boiling point of A-A; and second, a reduction in water evaporation, which helps preserve water and limit overall losses. In other words, the presence of A-A in the cooling and condensation section can provide a relative advantage for cooling system designers compared to conventional power plants.

It should be noted that, depending on the overall efficiency of the power plant, approximately 60% of the fuel's heating value is lost as waste heat in the condenser. Therefore, for the ammonia to be fully separated, the energy required for the separation process must be extracted from this available 60%; otherwise, complete separation of ammonia cannot be achieved. The lower the ammonia concentration in the A-A mixture, the higher the energy required for separation. In the

Table 13
Performance summary of the Rankine cycle at 100 °C condenser temperature.

Parameter	Value
Boiler Pressure (MPa)	16
High-Pressure Extraction (MPa)	4
Low-Pressure Extraction (MPa)	0.7
Condenser Pressure (MPa)	0.11
Boiler Outlet Temperature (°C)	540
Net Power Output (MW)	200
Mass Flow Rate (kg/s)	249.6
Condenser Mass Flow Rate (kg/s)	171.4
Fuel Mass Flow Rate (kg/s)	36.43
Extraction Fraction at FWH1 (–)	0.1497
Extraction Fraction at FWH2 (–)	0.1637
Boiler Heat Input (MW)	575.9
Condenser Heat Rejection (MW)	347.2
FWH1 Heat Transfer (MW)	75.98
FWH2 Heat Transfer (MW)	80.6
Turbine Total Work (MW)	205.6
Total Pump Work (MW)	5.65
Gross Thermal Efficiency (%)	34.73
Net Thermal Efficiency (%)	29.52

case of full evaporative separation (Method 1), energy is consumed to evaporate both ammonia and water entirely. Fig. 12 illustrates the performance of the power plant at various A-A concentrations, considering this energy constraint. It can be observed that at concentrations below 16%, there is insufficient energy available in the condenser to achieve complete separation, resulting in a drop in overall efficiency. This indicates that, under this design configuration, A-A with a minimum concentration of 16% should be used for energy transmission. Alternative separation methods or locating the separator within the boiler section can alleviate this constraint and allow for more flexibility in system design. This figure thus guides transport-concentration design choices: lower concentrations are feasible only when higher-grade heat or alternative separation methods are available.

In conclusion, if waste heat is to be used as the energy source for separation, the membrane method (Method 3) is the most appropriate. Furthermore, the separation process should be carried out at lower temperatures to maintain optimal plant performance.

5.2.2. Second scheme: supplying separation energy directly via fuel

In the second energy supply strategy, A-A serves as an intermediate medium to absorb heat. As ammonia separates from water, the remaining heat is transferred to the power cycle. The only loss involved is the energy required to break the ammonia-water bond—around 2.5% to 3.5% of the fuel's heating value—which is deducted from the transferred heat [34]. Unlike the first method, this loss reduces the input energy to the power cycle, lowering system efficiency.

The ideal location for the separator in this method is the boiler, which holds the highest temperature and energy level in the cycle. By placing the separator inside the boiler and transferring thermal energy first to the A-A and then to the working fluid, the full heating value of the fuel can be utilized.

According to Fig. 10, if the entire fuel heating value is available for separation (value of 1 on the graph), the minimum ammonia concentration required is reduced to 13% for Method 1 and 3% for Method 2. If minimizing fuel toxicity and corrosion is a design priority, these values can serve as criteria for fuel transport. However, lower concentrations imply higher water content in the transported fuel.

Although Method 2 (separator located in the boiler) allows use of all supply options and extends the range of acceptable A-A concentrations, exergy destruction during separation has a direct effect on overall plant efficiency.

Case 3 and 4 in Fig. 11 show thermal efficiency at two condenser pressures when the separator is in the boiler. The results indicate that a 2.5% to 3.5% energy loss causes a 1.2% to 1.5% efficiency reduction, depending on A-A concentration.

Despite this reduction, the benefits of using a clean fuel—such as environmental advantages and lower transportation and storage costs compared to NG or LNG—make this approach promising for A-A–based power plants.

5.3. Water transport with the fuel

Another key aspect of this system is the water transported with the fuel. Water is a critical resource in steam power plants, as it is required not only for steam generation but also for cooling, condensation, and various auxiliary processes. This dependency introduces significant limitations: plants located in water-scarce regions may face operational restrictions, efficiency losses can occur if cooling water is insufficient or warm, and environmental regulations may limit water withdrawal or discharge. In our case, using A-A as a combined fuel and water medium is particularly advantageous. Fig. 13 presents the modelled fuel and water consumption. To appreciate its significance, this transported water can be compared with typical water consumption in conventional power plants.

According to international standards (IEC 60193, ASME PTC 46), thermal power plant water consumption depends on the cycle type, cooling method, and environmental conditions. Studies by EPRI and DOE/NETL show that average water consumption for steam power plants with wet cooling systems ranges from 1.6 to 2.8 m^3/MWh, and for dry systems, from 0.1 to 0.2 m^3/MWh.

For instance, in the 205 MW case study plant operating under ISO conditions, calculations show required water flow rates of 91 to 159 kg/s for wet cooling, and 5.8 to 11.4 kg/s for dry cooling systems.

Fig. 13 quantifies the water mass co-delivered with A-A and compares it to the plant's cooling water demands. For a 15% A-A concentration, the transported water meets or exceeds wet cooling requirements (91–159 kg s^{-1}), thereby eliminating site water withdrawals. This result is one of the paper's most practical findings — A-A can simultaneously supply both energy and process water — but it is also contingent on the separation yield and local water-use permits if the produced water is to be diverted for non-process uses.

This system allows simultaneous transfer of fuel and water from energy- and water-rich regions (e.g., coastal areas) to inland power plants via pipelines. The waste or exchange energy in the cycle can be used to purify this water for the cooling system. Even when excess water is available, the produced water—nearly distilled—can be used for domestic or industrial purposes, with purification costs offset by waste heat from the plant.

5.4. Comparison with conventional power plants

To situate the present work within the existing body of research, a comparative assessment was conducted between this study and previously published investigations on ammonia- and hydrogen-based power generation systems. While past studies have explored combustion characteristics, cycle performance, or blended-fuel operation, none have examined aqua-ammonia as a fully integrated fuel system encompassing production, transport, separation, and steam-cycle combustion. Table 14 summarizes the key differences in scope, methodology, and achieved performance, highlighting the unique contributions and advancements introduced by the present work.

5.5. System sensitivity to design parameters

5.5.1. Boiler pressure effects

Boiler pressure was varied from 10 to 20 MPa to assess its influence on cycle performance. Results showed that increasing boiler pressure improves thermal efficiency due to a greater enthalpy drop across the turbine. Gross efficiency improved from 39.33% at 10 MPa to 42.02% at 20 MPa. However, the rate of improvement diminished beyond 18–19

Table 14
Comparison of this study with previous ammonia- and hydrogen-based power plant studies.

Study	Fuel	System type	Key efficiency/ findings	Limitations
Park et al. [21]	NH_3/ CH_4/H_2 blends	Gas turbine	Efficiency ~37–39%	No water synergy; pipeline challenges
Pashchenko (2022) [24]	NH_3	Recuperated GT	~35% efficiency	High NOx; requires recuperation
Shen et al. [23]	NH_3 + CO_2 cycle	Hybrid	~38%	Complex cycle; no transport analysis
Present work	A-A → NH_3	Rankine cycle	41.26–42.78%, water co-delivery; uses existing pipelines	Small separation penalty only (~1.2%)

MPa, indicating thermodynamic saturation and increased mechanical stress, which limit practical boiler pressure.

5.5.2. Condenser pressure effects

Lowering the condenser pressure increases the turbine expansion ratio, enhancing overall cycle efficiency. A reduction from 20 kPa to 5 kPa increased gross thermal efficiency from 39.57% to 42.78%. However, operating at very low condenser pressures (<8 kPa) introduces technical challenges, including the need for larger surface area condensers and more sophisticated vacuum systems.

5.5.3. Steam extraction pressure effects

Increasing the extraction pressure in both FWHs improved feedwater heating but reduced the energy available for turbine expansion. For the low-pressure heater, efficiencies slightly declined when extraction increased from 400 to 1200 kPa. Similarly, high-pressure extraction beyond 4000 kPa led to diminishing returns and a net reduction in turbine output. Optimal extraction pressures were thus identified around 4000 kPa (high-pressure) and 700 kPa (low-pressure).

6. Environmental impact assessment

The environmental performance of A-A–fuelled steam power plants is assessed in terms of greenhouse gas emissions, air pollutants, water consumption, and lifecycle sustainability. While ammonia combustion itself is carbon-free, its upstream production pathway and combustion byproducts determine its net environmental impact.

6.1. Greenhouse gas emissions

Unlike fossil fuels, ammonia combustion does not release CO_2 at the point of use. However, the total carbon footprint depends heavily on the source of ammonia:

- **Gray ammonia**, produced via the Haber-Bosch process using NG, emits between 1.8 and 3.0 kg CO_2 per kg of ammonia.
- **Blue ammonia**, produced similarly but with CCS, reduces emissions by up to 90%.
- **Green ammonia**, synthesized using renewable electricity and electrolysis, is virtually carbon-free.

At a fuel consumption rate of 30.66 kg/s and 8000 annual operating hours, the total annual ammonia requirement is approximately 773,000 t. Using gray ammonia results in annual CO_2 emissions of roughly 1.4 to 2.3 million tonnes—comparable to the emissions of 400,000 to 600,000 gasoline vehicles. By contrast, using green ammonia would eliminate this footprint entirely, enabling full decarbonization.

6.2. Combustion emissions: NO_x and N_2O

Although ammonia does not contain carbon, its combustion can lead to the formation of nitrogen-based pollutants:

- **NO_x emissions** occur due to high-temperature oxidation of atmospheric nitrogen and fuel-bound nitrogen. These can be mitigated through lean-premixed combustion, flue gas recirculation, and selective catalytic reduction systems.
- **N_2O emissions**, a potent greenhouse gas with 298 times the global warming potential of CO_2, may form under suboptimal combustion conditions. Maintaining high combustion efficiency and proper burner design can suppress its formation.

Ammonia slip (unburned ammonia in the exhaust) is also a concern but can be reduced to <10 ppm through optimized stoichiometry and excess air control.

6.3. Lifecycle sustainability and carbon reduction pathway

The long-term sustainability of the A-A system hinges on transitioning from gray to green ammonia. A phased implementation approach enables gradual emissions reductions:

1. **Short-term (gray ammonia)**: Leverages existing production and distribution systems. Emissions are shifted from the point of use to centralized production sites, where CCS is more feasible.
2. **Mid-term (blue ammonia)**: CCS-equipped production plants reduce the carbon intensity of fuel supply without changing combustion equipment.
3. **Long-term (green ammonia)**: Powered by solar or wind-based electrolysis, enabling a zero-emissions energy cycle.

This evolution mirrors the broader energy transition roadmap, in which fossil fuel infrastructure is repurposed rather than discarded, ensuring a just and economically viable transition.

7. Implementation strategy and future outlook

The proposed A-A system has several direct practical applications:

- Decarbonization of existing steam power plants without major redesign.
- Repurposing of existing NG pipelines for safe energy/water co-transport.
- Eliminating freshwater dependency for inland power plants through water delivered with A-A.
- Enabling fuel transport from coastal ammonia-production hubs to remote inland demand centres.
- Providing a scalable clean-fuel pathway compatible with green ammonia production.

Transitioning to A-A as a mainstream fuel for thermal power generation requires a phased and pragmatic approach, particularly in the context of entrenched fossil fuel infrastructure. This section outlines both the near-term deployment strategy and long-term vision for scalable, sustainable adoption.

7.1. Phased implementation pathway

The global NG supply chain represents a multi-trillion-dollar infrastructure investment, including pipelines, compressors, storage systems, and end-use appliances. Any disruptive alternative must minimize capital risk, align with existing regulatory frameworks, and provide

measurable environmental or economic advantages.

The proposed A-A system addresses these requirements by offering a phased transition through the following stages:

- **Phase 1 – Gray Ammonia Pilot Projects**: Initial deployment in remote, gas-importing regions where gray ammonia is economically favorable compared to liquefied NG (LNG). These projects can validate the technical model and build industrial expertise.
- **Phase 2 – Blue Ammonia Scaling**: As CCS technologies mature, blue ammonia becomes a more sustainable option. Retrofitting ammonia production plants with CCS will allow wider deployment in urban and industrial areas with modest investment.
- **Phase 3 – Green Ammonia Expansion**: With declining costs of renewable electricity and electrolysis, green ammonia becomes the default production route. This stage achieves true decarbonization of the fuel cycle and aligns with net-zero targets.

Each phase retains compatibility with the same infrastructure, allowing gradual fuel substitution without disrupting supply continuity.

7.2. Regional deployment flexibility

Unlike hydrogen, which demands significant infrastructure upgrades, A-A allows for localized deployment without altering broader gas grids. Ammonia and water can be transported by tanker, rail, or pipeline to regional hubs, where they are blended into A-A and distributed to power generation facilities. This modularity supports adoption in both developed and developing regions.

Inland power plants, often constrained by limited water access, benefit especially from A-A's dual fuel-and-water delivery capability. This decentralization also supports rural electrification and industrial decarbonization without overloading central utility networks.

7.3. Integration with renewable and circular systems

A-A is well-positioned to integrate with broader decarbonization efforts:

- **Solar-assisted ammonia production** reduces lifecycle emissions and aligns with countries possessing high solar irradiance.
- **Waste heat recovery** from industrial processes or power plant exhaust can support ammonia-water separation, improving overall system efficiency.
- **Water reuse** from the A-A separation cycle can serve agricultural, residential, or industrial needs, enhancing water resource circularity.

By embedding itself within renewable, waste-heat, and water conservation systems, A-A contributes to not only energy decarbonization but also climate resilience and resource efficiency.

8. Concluding remarks

This study demonstrates, with quantitative rigor and system-level modelling, the viability of A-A as a transformative fuel for decarbonizing steam-based thermal power generation. Beyond serving as a clean alternative to NG, A-A introduces a dual-function energy and water transport mechanism—a unique capability missing in other alternative fuels like hydrogen or pure ammonia.

Key findings of this study are summarized as follows:

- The proposed A–A–fuelled Rankine cycle achieved a gross thermal efficiency of 41.26–42.78%, exceeding comparable NG-fired systems.
- A 15% A-A mixture delivers ~3× the volumetric energy of NG in existing pipelines.
- The membrane-based separation method limits efficiency losses to only ~1.2%, the lowest among all examined options.
- Annual ammonia requirement of ~773,000 t enables near-zero CO_2 emissions when using green ammonia.
- Annual CO_2 reduction potential of up to 2.3 million tonnes when using green ammonia.
- Water transported with a 15% A-A mixture fully meets the plant's cooling and process water demand, eliminating external water dependency.

Through detailed thermodynamic simulations of a 200 MW Rankine cycle, the proposed system achieves gross thermal efficiencies exceeding 41% and net efficiencies above 35%, outperforming comparable fossil-fuelled systems while requiring only two open feedwater heaters. These results validate the technical feasibility of ammonia-fuelled cycles at utility scale with minimal infrastructure complexity. Moreover, system Optimisation across turbine efficiency, boiler pressure, condenser conditions, and part-load operation reveals that gross efficiency can be increased to 42.78%, with corresponding reductions in fuel consumption and emissions.

A key innovation is the use of A-A as a transport medium, allowing safe, low-pressure distribution through repurposed NG pipelines. A 15% A-A mixture can deliver up to three times the energy content of NG per unit volume, while simultaneously providing sufficient high-purity water for plant operation—eliminating dependence on local water sources and enhancing viability in arid or inland regions.

Importantly, the paper addresses the thermodynamic penalties associated with separating ammonia from water, evaluating three methods (evaporative, boiling-based, membrane) and proposing integration schemes that use either waste heat or direct fuel energy. The membrane-based separation method (M3), when coupled with condenser heat recovery, imposes negligible efficiency loss (~1.2%), while preserving process safety and system simplicity. Even under conservative design scenarios, total separation losses remain within 2.5–3.5% of the fuel's heating value, confirming the practicality of the approach.

From an environmental standpoint, ammonia combustion is carbon-free at the point of use, and the system's lifecycle emissions depend on the ammonia production route. Transitioning from gray to blue and ultimately green ammonia offers a clear decarbonization pathway. At full load, the plant consumes ~773,000 t of ammonia annually, which—if sourced from green pathways—could eliminate up to 2.3 million tonnes of CO_2 emissions per year, equivalent to removing over 500,000 vehicles from the road.

Beyond power generation, this A-A system presents a platform for multifunctional energy infrastructure. It integrates clean combustion, thermal storage, water distribution, and grid flexibility into a single carrier fluid. The ability to co-transport water and fuel is especially valuable for decentralized energy systems, coastal-to-inland energy transfer, and regions with water scarcity.

The novelty of this work lies in providing the first integrated assessment of A-A as a full-scale fuel—covering production, transport, separation, and combustion—and in introducing the dual energy–water delivery concept, which is absent in existing ammonia and hydrogen literature. This study also presents the first thermodynamic evaluation of a utility-scale Rankine cycle powered by ammonia extracted from A-A and demonstrates how membrane-based separation can be seamlessly integrated using condenser heat recovery.

In conclusion, A-A emerges not only as a safer and more scalable energy vector than hydrogen or pure ammonia, but also as a systems-level enabler for decarbonized power, resilient infrastructure, and sustainable resource integration. By addressing the critical research gap surrounding A-A's practical deployment, this work establishes a novel blueprint for immediate pilot implementation and a clear pathway toward net-zero power generation. This study provides a blueprint for immediate pilot deployment, while outlining a scalable path to net-zero

emissions through established ammonia technologies and infrastructure. As the global energy transition accelerates, the A-A approach offers a rare combination of technical maturity, economic feasibility, safety, and environmental impact—positioning it as a next-generation solution for clean, reliable, and sustainable thermal power. In addition to serving as a clean fuel solution for power plants, this approach offers a significant advantage in terms of providing an economical and environmentally low-impact water supply. It introduces unique capabilities specifically suited to steam power plants.

CRediT authorship contribution statement

Ramin Mehdipour: Writing – review & editing, Writing – original draft, Validation, Supervision, Software, Project administration, Methodology, Investigation, Formal analysis, Conceptualization. **Zahra Baniamerian:** Writing – review & editing, Validation, Software, Methodology, Investigation, Formal analysis, Data curation. **Hassan Ali Ozgoli:** Writing – original draft, Software, Methodology, Formal analysis, Data curation. **Seamus Garvey:** Writing – review & editing, Supervision, Resources, Project administration, Funding acquisition. **Alasdair Cairns:** Writing – review & editing. **Agustin Valera-Medina:** Writing – review & editing. **Sivachidambaram Sadasivam:** Writing – review & editing. **Bruno Cardenas:** Writing – review & editing.

Declaration of competing interest

The authors declare that they have no known competing financial interests or personal relationships that could have appeared to influence the work reported in this paper.

Acknowledgements

The authors would like to thank the United Kingdom's Engineering and Physical Sciences Research Council (EPSRC) for supporting this work through the EPSRC IAA Impact Exploration Grant. Project code: EP/X525765/1.

Data Access Statement: No new experimental or observational data were generated in this study. All results were obtained from deterministic energy system simulations using parameters and assumptions fully described within the article.

Data availability

Data will be made available on request.

References

[1] L. Liu, C. Xu, Y. Yang, C. Fu, F. Ma, Z. Zeng, Graphene-based polymer composites in thermal management: materials, structures and applications, Mater. Horiz. 12 (2025) 64–91.
[2] A. Mirahmad, R.S. Kumar, B.P. Doldán, C. Prieto Rios, J. Díez-Sierra, Beyond thermal conductivity: a review of nanofluids for enhanced energy storage and heat transfer, Nanomaterials 15 (4) (2025).
[3] A. Borode, T. Tshephe, P. Olubambi, A critical review of the thermophysical properties and applications of carbon-based hybrid nanofluids in solar thermal systems, Front. Energy Res. 12 (2025).
[4] Thermophysical properties of nanofluids and their potential applications in heat transfer enhancement: a review, Arab. J. Chem. (2023).
[5] doi: https://doi.org/10.1016/C2022-0-02476-4.
[6] Int. J. Hydrog. Energy 47 (8) (2022) 5403–5417.
[7] Z. Baniamerian, R. Mehdipour, C. Aghanajafi, Analytical simulation of annular two-phase flow considering the four involved mass transfers, J. Fluids Eng. 134 (8) (2012) 081301, https://doi.org/10.1115/1.4005949.
[8] Z. Baniamerian, C. Aghanajafi, Studying the influence of refrigerant type on thermal efficiency of annular two-phase flows; mass transfer viewpoint, Korean J. Chem. Eng. 28 (2011) 49–55, https://doi.org/10.1007/s11814-010-0333-1.
[9] M.M. Mohebali, Z. Baniamerian, Effect of nanofluid sedimentation on heat transfer and critical heat flux in boiling flows, J. Therm. Anal. Calorim. 149 (2024) 8225–8244, https://doi.org/10.1007/s10973-024-13303-4.
[10] H. Azimi, Z. Baniamerian, Effects of nanoparticles deposition on thermal behaviour of boiling nanofluids, Heat Mass Transf. 55 (2019) 105–117, https://doi.org/10.1007/s00231-018-2353-z.
[11] Mehdi Mousavi-Kamazani, Mohammd Ghodrati, Sahar Zinatloo-Ajabshir, The impact of hollow sphere architecture on improved hydrogen storage performance of hydrothermally synthesized zinc vanadate, J. Energy Storage, volume 132, Part C, 2025, 117974.
[12] Maryam Hasanzadeh Esfahani, Sahar Zinatloo-Ajabshir, Hojjat Naji, Casey A. Marjerrison, John E. Greedan, Mahdi Behzad, Structural characterization, phase analysis and electrochemical hydrogen storage studies on new pyrochlore SmRETi2O7 (RE = Dy, ho, and Yb) microstructures, Ceram. Int. 49 (1) (2023) 253–263.
[13] J. Gallagher, Hydrogen storage: pressure swing, Nat. Energy 2 (7) (2017), https://doi.org/10.1038/nenergy.2017.122.
[14] J. Ogden, A.M. Jaffe, D. Scheitrum, Z. McDonald, M. Miller, Natural gas as a bridge to hydrogen transportation fuel: insights from the literature, Energy Policy 115 (2018) 317–329, https://doi.org/10.1016/j.enpol.2017.12.049.
[15] D. Haeseldonckx, D'haeseleer, W., The use of the natural-gas pipeline infrastructure for hydrogen transport in a changing market structure, Int. J. Hydrog. Energy 32 (10–11) (2007) 1381–1386, https://doi.org/10.1016/j.ijhydene.2006.10.018.
[16] S. Chaturvedi, R. Santhosh, S. Mashruk, R. Yadav, A. Valera-Medina, Prediction of NOx emissions and pathways in premixed ammonia-hydrogen-air combustion using CFD-CRN methodology, J. Energy Inst. 111 (2023) 101406, https://doi.org/10.1016/j.joei.2023.101406.
[17] M. Melaina, M. Penev, J. Zuboy, Hydrogen blending in natural gas pipelines, in: Handbook of Clean Energy Systems, 2015, pp. 1–13, https://doi.org/10.1002/9781118991978.hces205.
[18] M. Sofian, M.B. Haq, D.A. Shehri, M.M. Rahman, N.S. Muhammed, A review on hydrogen blending in gas network: insight into safety, corrosion, embrittlement, coatings and liners, and bibliometric analysis, Int. J. Hydrog. Energy 60 (2024) 867–889, https://doi.org/10.1016/j.ijhydene.2024.02.166.
[19] Z. Cai, M. Huang, G. Wei, Z. Liu, H. Zhang, Q. Hao, Z. Yu, Theoretical study on the inherent relationship between laminar burning velocity, ignition delay time, and NO emission of ammonia-syngas-air mixtures under gas turbine conditions, Int. J. Hydrog. Energy 50 (2024) 690–705, https://doi.org/10.1016/j.ijhydene.2023.11.088.
[20] International Energy Agency, The Role of Low-carbon Fuels in the Clean Energy Transitions of the Power Sector, OECD Publishing, 2021, https://doi.org/10.1787/a92fe011-en.
[21] Y. Park, M. Choi, G. Choi, Thermodynamic performance study of large-scale industrial gas turbine with methane/ammonia/hydrogen blended fuels, Energy 282 (2023) 128731, https://doi.org/10.1016/j.energy.2023.128731.
[22] R. Ślefarski, P. Czyżewski, M. Gołębiewski, Experimental study on combustion of CH4/NH3 fuel blends in an industrial furnace operated in flameless conditions, Therm. Sci. 24 (6 Part A) (2020) 3625–3635, https://doi.org/10.2298/tsci200401282s.
[23] Z. Shen, S. Liang, K. Chen, Y. Zhu, B. Wang, Analysis of cyclic thermodynamic system combining ammonia gas turbine and transcritical carbon dioxide, Appl. Energy 376 (2024) 124238, https://doi.org/10.1016/j.apenergy.2024.124238.
[24] D. Pashchenko, R. Mustafin, I. Karpilov, Ammonia-fired chemically recuperated gas turbine: thermodynamic analysis of cycle and recuperation system, Energy 252 (2022) 124081, https://doi.org/10.1016/j.energy.2022.124081.
[25] N.A. Hussein, A. Valera-Medina, A.S. Alsaegh, Ammonia- hydrogen combustion in a swirl burner with reduction of NOx emissions, Energy Procedia 158 (2019) 2305–2310, https://doi.org/10.1016/j.egypro.2019.01.265.
[26] X. Shi, T. Lian, Y. Zhang, Z. Liu, W. Li, Z. Xi, Y. Li, Enhanced ammonia combustion by partial pre-cracking strategy in a gas turbine model combustor: flame macrostructures, lean blowout characteristics and exhaust emissions, Appl. Energy Combust. Sci. (2024) 100247, https://doi.org/10.1016/j.jaecs.2024.100247.
[27] A. Valera-Medina, F. Amer-Hatem, A.K. Азад, I.C. Dedoussi, M. De Joannon, R. X. Fernandes, P. Glarborg, H. Hashemi, X. He, S. Mashruk, J. McGowan, C. Mounaim-Rouselle, A. Ortiz-Prado, A. Ortiz-Valera, I. Rossetti, B. Shu, M. Yehia, H. Xiao, M. Costa, Review on Ammonia as a potential fuel: from synthesis to economics, Energy Fuel 35 (9) (2021) 6964–7029, https://doi.org/10.1021/acs.energyfuels.0c03685.
[28] M. Alnajideen, H. Shi, W. Northrop, et al., Ammonia combustion and emissions in practical applications: a review, Carbon Neutrality 3 (2024) 13, https://doi.org/10.1007/s43979-024-00088-6.
[29] A. Rusin, K. Stolecka-Antczak, Assessment of the safety of transport of the natural gas–ammonia mixture, Energies 16 (5) (2023) 2472, https://doi.org/10.3390/en16052472.
[30] Y.Y. Liu, G.Z. Quan, Y.Z. Yu, W.J. Ran, W. Xiong, Corrosion behaviors of Ni80A alloy valve in marine engine within ammonia-rich environment, Materials (Basel) 18 (13) (2025) 3006, https://doi.org/10.3390/ma18133006. PMID: 40649494; PMCID: PMC12251521.
[31] M.R. Shahrokhi, H.A. Ozgoli, F. Farhani, Comparative analysis of a dual Kalina cycle configuration for heat recovery from boiler stack in a steam power plant, Environ. Prog. Sustain. Energy 41 (6) (2022) e13900, https://doi.org/10.1002/ep.13900.
[32] M. Hosseinpour, H.A. Ozgoli, S.A. Hajiseyed Mirzahosseini, A.H. Hemmasi, R. Mehdipour, Evaluation of performance improvement of the combined biomass gasifier power cycle using low-temperature bottoming cycles: organic Rankine cycle, Kalina and Goswami, Environ. Prog. Sustain. Energy 41 (5) (2022) e13855, https://doi.org/10.1002/ep.13855.
[33] M. Hosseinpour, H.A. Ozgoli, S.A. Haji Seyed Mirza Hosseini, A.H. Hemmasi, R. Mehdipour, Energy analysis of utilizing biomass gasification to partially substitution fossil fuels in an IBG-GT-ST-Kalina cycle, J. Renew. Energy Environ. 9 (3) (2022), https://doi.org/10.30501/jree.2022.321835.1307.

[34] R. Mehdipour, Z. Baniamerian, S. Garvey, Thermal performance assessment of aqua-Ammonia in space heating applications, Appl. Therm. Eng. 279 (E) (2024) 127906, doi:10.1016/j.applthermaleng.2025.127906.
[35] R. Mehdipour, S. Garvey, Z. Baniamerian, B. Cardenas, Ice source heat pump system for energy supply via gas pipelines – Part1: performance analysis in residential units, Energy (2024) 132974, https://doi.org/10.1016/j.energy.2024.132974.
[36] R. Mehdipour, S. Garvey, Z. Baniamerian, B. Cardenas, A comparative study on the performance of ice-source heat pumps versus other heat source heat pumps: a case study in the UK, Renew. Energy (2024) 121867, https://doi.org/10.1016/j.renene.2024.121867.
[37] R. Mehdipour, S. Garvey, B. Cardenas, Z. Baniamerian, C.J. Wood, Ice-source heat pump for residential heating: a case study on energy storage and pipeline repurposing in the UK, Case Stud. Therm. Eng. (2025) 106579, https://doi.org/10.1016/j.csite.2025.106579.
[38] R. Mehdipour, S. Garvey, Z. Baniamerian, B. Cardenas, Ice-source heat pumps: sustainable heating solutions for urban areas utilizing water and gas networks, Energ. Buildings 343 (2025) 115916, https://doi.org/10.1016/j.enbuild.2025.115916.
[39] Michaela Sommer, Matthias Steinbacher, Stefanie Hojam, Thermochemical corrosion of furnace materials in atmospheres containing Ammonia, Mater. Corros., **doi:**https://doi.org/10.1002/maco.202414499**.**
[40] J. Phys. Chem. Ref. Data Monogr. 27 (1998) 63, https://doi.org/10.1063/1.556015.
[41] C.L. Sassen, R.A.C. Van Kwartel, H.J. Van der Kooi, J. De Swaan Arons, J. Chem. Eng. Data 35 (2) (1990) 140–144, https://doi.org/10.1021/je00060a013.
[42] Thermodynamic analysis of a power cycle using a low-temperature source and a binary NH3–H2O mixture as working fluid, Int. J. Therm. Sci. 49 (1) (2010) 48–58.
[43] Thermodynamic performance assessment of an ammonia–water Rankine cycle for power and heat production, Energy Convers. Manag. 51 (12) (2010) 2501–2509.
[44] Robert W. Serth, Thomas G, in: Lestina, PROCESS HEAT TRANSFER PRINCIPLES, APPLICATIONS AND RULES OF THUMB, Second edition, Elsevier publishing, 2014.
[45] K.M. Mohammed, W.H. Al Doori, A.H. Jassim, T.K. Ibrahim, A.T. Al-Sammarraie, Energy and exergy analysis of the steam power plant based on effect of the numbers of feed water heater, J. Adv. Res. Fluid Mech. Therm. Sci. 56 (2) (2019) 211–222.
[46] H.G. Ibrahim, M.S. Elatrash, A.Y. Okasha, Steam power plant design upgrading (case study: Khoms steam power plant), Energy Environ. Res. 1 (1) (2011) 202–211, https://doi.org/10.5539/eer.v1n1p202.